WARWICK

ECONOMICS

CRETA

Centre for Research in Economic Theory and its Applications

Discussion Paper Series

Market Instability, Investor Sentiment, And Probability Judgment Error in Index Option Prices

G. Charles-Cadogan

May 2021 No: 71

CRETA
Centre for Research in Economic Theory and its Applications
Department of Economics
University of Warwick, Coventry,
CV4 7AL, United Kingdom

warwick.ac.uk/fac/soc/economics/research/centres/creta/papers

Market Instability, Investor Sentiment, And Probability Judgment Error in Index Option Prices[*]

G. Charles-Cadogan [†]

Working paper
Comments welcome

May 11, 2021

Abstract

In a natural experiment with index option prices, we study how probability judgment error, and probabilistic risk attitudes, characterize investors' sentiment about the ranking of index option attractiveness, the weight they place on each rank, and their ability to discriminate between prices. We introduce a novel behavioral process that (1) characterizes investor sentiment about tail events in index option prices over time and probability ranks, (2) provides early warning signals of market instability, and (3) crash probability estimates from a closed form expression for the time varying transition probability that a seemingly stable market state will become unstable and crash.

Keywords: sentiment, crash risk, probability weighting function, index option prices, market instability

JEL Classification Codes: C02, C44, D03, D81, G01, G12

[*]This paper benefitted from discussions with Paul Dunne and Amos Peters. I thank Gana Pogrebna, Zvi Wiener, Christie Schoeman, John Mwamba, Pablo Brañas Garza, Haim Abraham, Emmanuel Haven, Sandro Sozzo, Nikolaos Vlastakis, Vivekanand Nawosah, Jerry Coakley, Andrew Coleman, Briony Pulford, Radu Tunaru, Mohamed Hasan, Timothy King, Jaideep Oberoi and seminar participants at the University of Johannesburg, University of Leicester, University of Cape Town, University of Essex, University of Kent, and International Risk Management Conference (IRMC) SDA Bocconi for their comments on earlier versions of this paper. I thank Svetlozar Rachev for bringing my attention to related work, and Sure Mataramvura for a thorough reading of the manuscript, and Peter Wakker for detailed comments. Any errors which may remain are my own.

[†]University of Leicester, School of Business, Division of Finance, Brookfield Campus, Leicester, LE2 1RQ; Tel: +44 (0116) 229 7385; and Institute for Innovation and Technology Management (IITM), Ted Rogers School of Management, Ryerson University, 575 Bay, Toronto, ON M5G 2C5; e-mail: gcc13@le.ac.uk

Contents

List of Figures

List of Tables

1 Introduction

The burgeoning literature on investor sentiment[1] and market psychology is dense with keywords and phrases like: hope, fear, aspirations, underconfidence and overconfidence, investors risk attitudes toward tail events, and formation of asset pricing bubbles. All of the above can be characterized by "probability judgment error"[2] (see e.g. Dierkes et al., 2020; Baele et al., 2019; He and Zhou, 2016; Kuhnen, 2015; Wigniolle, 2014; Polkovnichenko and Zhao, 2013; Dierkes, 2013; Chabi-Yo and Song, 2013; Kliger and Levy, 2010; Dierkes, 2009; Ackert et al., 2009; Haigh and List, 2005; Kluger and Wyatt, 2004; Fox et al., 1996). Psychological probability, by and through the probability weighting function component of rank dependent utility and prospect theory (Quiggin, 1982, 1993; Lopes, 1987, 1990; Tversky and Kahneman, 1992), plays a key role in evaluating probability judgment error in many of those papers.

In a natural experiment with index option prices, we investigate an unexplored area of probability judgment error in financial markets. Namely, financial market instability driven by probabilistic sentiment.[3] We study *how* probabilistic sentiment characterizes financial market switch from states of optimism to pessimism and *vice versa*. We derive a closed form expression for the transition probability that a seemingly stable financial market will become unstable and crash because of sentiment driven probability judgment error. This allows us to estimate crash probabilities, critical values of a probability factor associated with attractiveness of an asset, and identify early warning signals of market crash (e.g. market surveillance). The novel approach in this paper stems from its representation of the term

[1] "Sentiment" is described as an "emotional reaction to risky situations that often diverge from cognitive assessments of those risks" (Loewenstein et al., 2001). Thus, investors' emotional response to associated risks in financial markets that deviate from cognitive models of market stability constitute investor sentiment or judgment error (cf., De Long et al., 1990).

[2] The extent to which probability judgment deviates from objective probability gives us a measure for sentiment. According to Barberis (2013, p. 176) "people do not weight outcomes by their objective probabilities p_i but rather by transformed probabilities or decision weights π_i. The decision weights are computed with the help of a [probability] weighting function $w(\cdot)$ whose argument is an objective probability."

[3] A notable exception is Ackert et al. (2009) who examine asset price bubbles induced by probability judgment error in an experimental market. This paper was written before the SARS-cov-19/COVID-19 pandemic that caused governments to shut down their economies globally. The pandemic is different from a market crash induced purely by investors' sentiment about assets attractiveness. Those dynamics are briefly described in Figure 20, *infra*. We note that without loss of generality the "financial market" in contention is one in which professional option traders are the actors.

structure of probability judgment error as a behavioral random field–constructed from noise

Figure 1: A random field of probability weighting functions impied by monthly S&P 500 index option

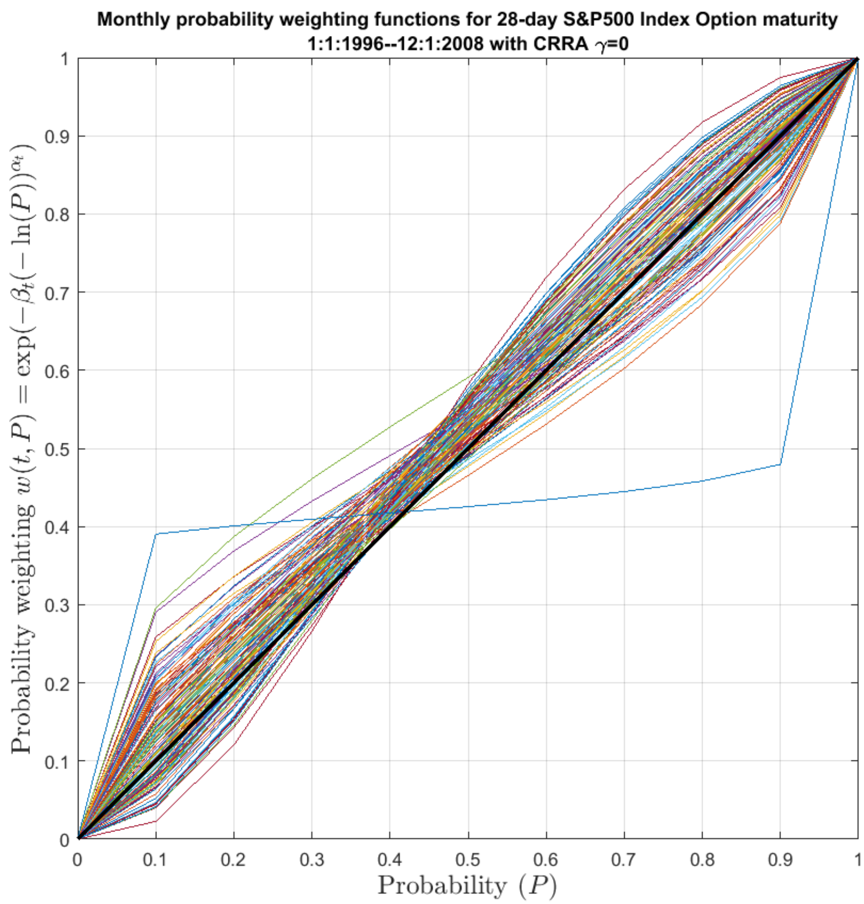

Source: Author's computation from data extrapolated from Polkovnichenko and Zhao (2013) for January 1996 to December 2008. The outlier curve reflects sentiment about the Great Recession of 2008.

in investors' probability judgment–continuous in time and measurable in probability ranks.[4] In the sequel we refer to this random field as a "BELLE process" even though that phrase typically applies to the time dependent component of the field. It is known that probability weighting functions reflect probability judgment error, and that they are measures of sen-

[4]Let $X_1, \ldots, X_n$ be a random sample of outcomes, i.e. prices, $X_{(n)}, \ldots, X_{(1)}$ be a ranking from low to high, P be a probability measure, and F the corresponding distribution function. $P(X < X_{(m)}) = F(X_{(m)}) = p_m$ implies that p_m is the probability rank of $X_{(m)}$.

timent (Barberis, 2013). Given professional option traders proneness to sentiment driven probability judgment error (Fox et al., 1996; Haigh and List, 2005), probability weighting functions (pwfs) implied by S&P 500 index option prices provides a natural experiment to evaluate the model's performance in well known financial crises. In Figure 1 the field of pwfs assume different shapes depending on the sources or states of risk that characterize the sample functions over probability ranks dimension for each time index in the data. We call these sample functions source functions in keeping with the nomenclature in prospect theory (Wakker, 2010; Abdellaoui et al., 2011). The shapes of source functions for index option prices reflect investors' sentiments about different sources of risk in the market. For example, new information about credit events such as mark-to-market write downs causes credit rating agencies to change credit ratings, i.e. credit ratings migration that re-rank credit worthiness (cf. Altman, 1998; Finnerty et al., 2013), and induce a new distribution of probability of default. This is followed by a change in market sentiment, i.e. re-evaluation of default probabilities, that consequently changes the shapes of source functions.[5]

We show that unstable and stable market states are characterized by convex-concave (S) and concave-convex (inverted S) shapes, respectively, for source functions. This enables us to identify transient shapes of source functions over time, and the critical limit shape when markets crash. For example, we derive critical values for a probability judgment index for attractiveness of index option prices. Those values show that markets crash when source functions transmogrify from inverse S-shape (or S-shape) into a tent map with upper vertex above the 50-50 probability mark.[6] To the best of our knowledge, this paper is the first to establish a nexus between probability judgment error and tent maps in financial markets

[5]Refer to Wang et al. (2017) for details on Moody's Credit Transition model. Yamazaki (2020) incorporated source functions and default probabilities in a consumption based asset pricing model (CCAPM) to explain why stocks of distressed firms have negative risk premium. Ismailescu and Kazemi (2010) used regression methods to find asymmetric sovereign credit market response to downgrade versus upgrade for emerging markets, whereas Drago and Gallo (2017) find asymmetric response in the opposite direction for developed European markets.

[6]Campbell et al. (1997, p. 474) describe the locus of a tent map. In our case, psychological probability $w(p_t)$ in index option markets collapsed to the following tent map when the market crashed in 2008:

$$p_t = \begin{cases} 2p_{t-1}, & p_{t-1} < 1/2; \\ 2(1-p_{t-1}), & p_{t-1} \geq 1/2; \end{cases} , \qquad p_0 \in (0,1)$$

(cf. Hsieh, 1991; Campbell et al., 1997; Brock and Hommes, 1998). Among other things, a tent map implies that investors exhibit extreme likelihood insensitivity, i.e. they are unable to discriminate among bets in the index option market, and they are extremely pessimistic about 50-50 bets on option prices due to unattractive toxic assets. For instance, the flat portion of the outlier plot in Figure 1 exhibits extreme likelihood insensitivity (Wakker, 2010, p. 203). Hence no trade takes place and markets crash. As we will see, just before the extreme likelihood insensitivity state is reached, source functions morph into latent tent maps.[7] So, the latter provide strong signals that the market will crash. For example, our model predicted tent map market crash states in July and August 2008–two months before the Lehman Brothers bankruptcy induced crash in September 2008. After the crash, source functions resumed concave-convex shapes consistent with probabilistic risk aversion. Jackwerth (2020, p. 624) showed that deformation of functional risk neutral probability dynamics on March 16, 2020 did a better job of anticipating the COVID-19 market crash on March 23, 2020 compared to the S&P500 index value.

The BELLE process admits a closed form expression for the time dependent probability that a seemingly stable financial market state will transit to an unstable state.[8] The model makes the fatalistic prediction that the market will become unstable and crash almost surely in finite time (cf. Kindleberger and Aliber, 2011). Somewhat surprising, when the volatility of probability judgment error is high, the probability of market instability is lower than when the volatility of probability judgment is low. Evidently, larger volatility for probability judgment error in index option market reflects larger differences of opinion about prices and it mitigates market instability (Chen et al., 2012; Carlé et al., 2019).

[7]The natural experiment data allows us to address Campbell et al. (1997, p. 475) observation that "[t]his technique, known as a *stroboscopic map* or a *Poincare section*, has given empirical content to even the most abstract notions of nonlinear dynamical systems, but unfortunately cannot be applied to non-experimental data."

[8]Schularick and Taylor (2012); Cesa-Bianchi et al. (2018) used a logit model of banking crisis with data for credit growth to estimate this probability but they did not use source functions.

Figure 2: Risk sources and investor psychology

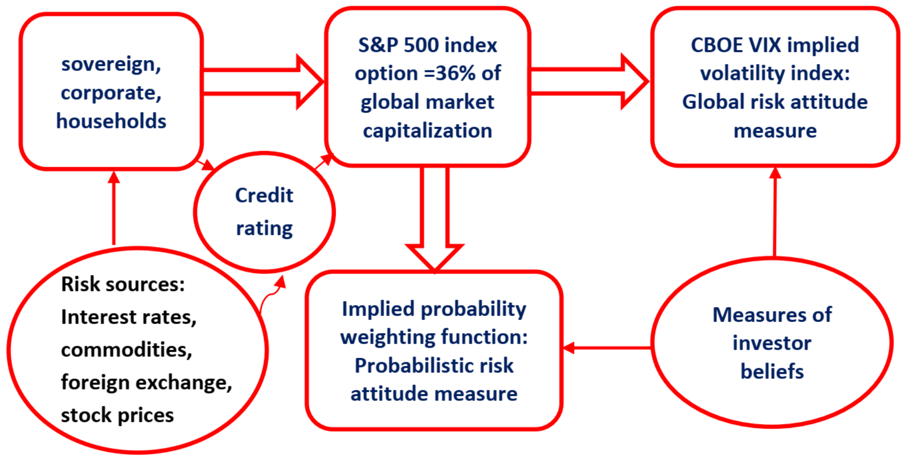

Figure 2 provides a *schema* of how investor beliefs about risk sources are transmitted to the CBOE VIX and the pwf implied by S&P 500 index option prices. According to Figure 2, the sources of risk affect sovereigns, corporations and households and consequently the cash flow streams anticipated by investors over a given time horizon. Information that impact risk assessment such as credit rating migration induce re-ranking of assets and probability redistribution that are reflected in the shapes of sources functions. Thus, investors probabilistic risk attitudes are time and source (state) dependent as indicated in Figure 1.[9] The CBOE VIX provides a volatility score for risk; whereas a risk source function, i.e. the pwf corresponding to the source of risk, reflects investors probabilistic risk attitudes and sentiment about the probability ranks of index option prices that produce the VIX score. Recently, Chabi-Yo and Song (2013) established a nexus between VIX scores and pwfs by showing how to recover pwfs nonparametrically from S&P 500 index option implied volatility and VIX options. Dierkes (2013) also provides a link between VIX and the curvature of source functions.

The rest of the paper proceeds as follows. In section 2 we provide a heuristic example of how investor sentiment affects option prices. We introduce the BELLE process which

[9]Refer to Baucells and Heukamp (2012); Savadori and Mittone (2015) for time varying probabilistic risk attitudes. The source dependence of pwfs (Tversky and Wakker, 1995; Kilka and Weber, 2001; Abdellaoui et al., 2011) provides insight about probabilistic risk attitudes that is lacking in raw VIX scores.

characterizes stability of source functions; closed form expressions for tipping points; and large deviation probabilities for source function shape reversal based on discrimination and attractiveness of option prices. In section 3 we calibrate the model to source functions corresponding to the sources of risk implied by S&P 500 index option prices, and show how they predict market crash and provide early warning systems for market instability. In section 4 we conclude.

2 The BELLE process for probability weighting functions

This section deals with how the BELLE process is derived.[10]. We consider the *finite-time* behaviour of the Lyapunov exponent for an orbit of probability weighting functions with behavioural error for a large sample of investors. Specifically, we characterize stable and unstable pwfs and the large sample probability estimate(s) for *tail event instability* in a seemingly stable system of investors' pwfs. We apply it in Section 3 to detect market crash phenomenon in option price data. The basin of attraction $B_\delta(p^\star)$ characterizes the stable and unstable pwfs for investors in the behavioral dynamical system (see Definition G.2 in the appendix) for pwfs based on an invariant manifold theorem (see Proposition 2 in appendix). At this point it is perhaps instructive to use an heuristic example to illustrate how the shape parameters affect option prices.

2.1 A heuristic example of how investor sentiment affects option prices

Assume that a European style call option price at time t with expiry date $T > t$ is a simple mixed lottery L, i.e. buy at K with time discount $e^{-r(T-t)}$ and probability P_2, sell at $S(t)$ with probability P_1. So, $L = \{S(t), P_1;\ -e^{-r(T-t)}K, P_2\}$. The actuarial value of L is a call option $C(S, K, \sigma, t, r) = S(t)P_1 - e^{-r(T-t)}KP_2$, where S is the underlying stock price, σ is its volatility, K is strike price, r is a constant discount rate, and T is expiry date, P_1 and

[10] BELLE stands for "behavioural empirical local Lyapunov exponent". A Lyapunov exponent (λ) is a measure of the rate of convergence or divergence of a trajectory over time relative to two nearby starting points

P_2 are probabilities. In Heston (1993, pp. 330,331) option pricing model P_1 and P_2 can be sub(super)-additive (cf., Fox et al., 1996) and they depend on arguments of the call option.[11]

Motivated by Shefrin and Statman (1993, p. 125, fn 4), we assume out-of-the-money call option valuation with psychological probabilities. We use Prelec's (1998) sub(super)-additive 2-parameter probability weighting function

$$w(P) = \exp\left(-\beta(-\ln(P))^{\alpha}\right) \tag{2.1}$$

to replace the objective probabilities in the actuarial value of L to obtain a behavioural value

$$\widetilde{C}(S, \sigma, t, r;\, \alpha, \beta) = S(t)w(P) - e^{-r(T-t)}K(1 - w(1 - P)) \tag{2.2}$$

*** Insert Figure 3 and Figure 4 about here ***

Assume assets are ranked from worst to best, and $P_1 = w(P)$ and $P_2 = 1 - w(1 - P)$. (Pess)imists believe (P^{pess}): $P_1 = w(P) < P$ for high ranks, and $w(1 - P) < 1 - P$, so for them $P_1 < P < P_2$ for arbitrary P. (Opt)imists believe the opposite (P^{opt}): $P_1 > P$ and $P_2 < P$, so for them $P_1 > P > P_2$ for high rank assets. Thus, $P_1^{opt} > P_1^{pess}$ and $P_2^{opt} < P_2^{pess}$, i.e., $P_1^{opt} - P_1^{pess} > 0$ and $P_2^{opt} - P_2^{pess} < 0$. Substitution of these values in (2.2) results in $\widetilde{C}^{opt}(\cdot;\, \alpha^{opt}, \beta^{opt}) > \widetilde{C}^{pess}(\cdot;\, \alpha^{pess}, \beta^{pess})$ as follows:

$$\widetilde{C}^{opt}(\bullet) = S(t)P_1^{opt} - e^{-r(T-t)}\, K\, P_2^{opt} \tag{2.3}$$

$$\widetilde{C}^{pess}(\bullet) = S(t)P_1^{pess} - e^{-r(T-t)}\, K\, P_2^{pess} \tag{2.4}$$

$$\widetilde{C}^{opt}(\bullet) - \widetilde{C}^{pess}(\bullet) = S(t)(P_1^{opt} - P_1^{pess}) - e^{-r(T-t)}\, K\, (P_2^{opt} - P_2^{pess}) \tag{2.5}$$

$$= \overbrace{S(t)(P_1^{opt} - P_1^{pess})}^{+\text{ve}} + \overbrace{e^{-r(T-t)}\, K\, (P_2^{pess} - P_2^{opt})}^{+\text{ve}} > 0 \tag{2.6}$$

[11]In Heston (1993) $P_1 + P_2 = 1 + \frac{1}{\pi}\int_0^{\infty} \frac{e^{-i\phi \ln[K]}}{i\phi}\left(\mathrm{Re}(\widehat{\mathfrak{f}}_1) + \mathrm{Re}(\widehat{\mathfrak{f}}_2)\right) d\phi$ where $\widehat{\mathfrak{f}}_j$ is the characteristic function of P_j, $j = 1, 2$. If the integrand is not zero, then $P_1 + P_2 \neq 1$ so the probability measures are super(sub)-additive accordingly. Note that $P_1 = N(d_1)$ and $P_2 = N(d_2)$ in the Black and Scholes (1973) formula.

Markets breakdown when the inequality in (2.6) fails, i.e., optimist valuation of the call option is at most equal to the pessimist valuation: $\widetilde{C}^{opt}(\cdot;\, \alpha^{opt}, \beta^{opt}) \leq \widetilde{C}^{pess}(\cdot;\, \alpha^{pess}, \beta^{pess})$. Here, α, β reflect investor sentiment: α curvature is an index for discrimination of bet on option prices, and β elevation is an index for attractiveness of option prices. See Gonzalez and Wu (1999) for further psychological interpretation of α and β. Each of the two components in (2.6) depend on probabilistic risk attitudes.

Let $Mood(S) = S(t)(P_1^{opt} - P_1^{pess})$ and $Mood(K) = e^{-r(T-t)}\, K\, (P_2^{pess} - P_2^{opt})$.

Pessimism If market $Mood(S)$ is overly pessimistic about S (e.g., during and after rare disaster (cf. Giglio et al., 2021, p. 1484)) such that $P_1^{pess} \gg P_1^{opt}$ and $Mood(S) \ll 0$, $Mood(K)$ held constant, and $Mood(S) + Mood(K) \leq 0$, then markets fail.

Exuberance If market $Mood(K)$ is overly optimistic about K (e.g., long shot bias about lottery stocks (cf., Snowberg and Wolfers, 2010)) such that $P_2^{pess} \ll P_2^{opt}$ and $Mood(K) \ll 0$, $Mood(S)$ is held constant, and $Mood(S) + Mood(K) \leq 0$, then markets fail.

Mood disparity If $Mood(S) + Mood(K) \leq 0$, then markets fail.

Figure 3 and Figure 4 depict optimist and pessimist likelihood insensitivity for a true probability weight $\Delta P = 0.1$ over P-ranks and over time. There, one can see a probability smile (for pessimists) and probability frown (for optimists). For likelihood insensitivity, the optimist overweighs and the pessimist underweighs the true ΔP. This overweighing phenomenon in optimistic states (in our case option prices with high probability ranks) was recently confirmed in Akbas and Genc (2020, p. 225) for the case of mutual funds.

2.2 Stable and unstable probability weighting functions in index options market

The phase diagrams in Figure 5 and Figure 6 show the stable manifold theorem (Theorem G.1) at work in the interior fixed point for stable and unstable source functions implied by index options.[12] In particular, concave-convex shapes are stable, and convex-concave

[12] Roughly, the stable manifold theorem characterizes the (in)stability of the system in a neighbourhood of the fixed point.

shapes are unstable. The latter is characteristic of "irrational exuberance" in financial markets. This paper shows how the source functions are oriented just before, during, and after a market crash.

*** Insert Figure 5 and Figure 6 about here ***

2.3 Local Lyapunov exponent for probability weighting functions

In this subsection we formally define and identify the Lyapunov exponent for pwfs. Intuitively, a Lyapunov exponent λ is a measure of the rate of system divergence from or convergence to an equilibrium when two nearby initial conditions are perturbed.

Definition 2.1 (Lyapunov exponent)**.** Adapted from Jost (2005, pg. 31). Let $w(p)$ be a probability weighting function such that the first derivative w' exist. The Lyapunov exponent of the orbit $p_n = w(p_{n-1}),\ n \in \mathbb{N}$ for $p_0 = p$ is

$$\lambda(p) := \lim_{n\to\infty} \frac{1}{n} \sum_{j=1}^{n} \ln |w'(p_j)| \tag{2.7}$$

provided the limit exist. $\square$

This definition implies that the Lyapunov exponent is an invariant of the Jacobian $w'(p_j) = \frac{\partial w}{\partial p_j}$ that determines local stability of the points that satisfy (2.7). It is the average rate of divergence for the *iterative function system* p, $w(p)$, $w \circ w(p), \ldots, w \underbrace{\circ \ldots \circ}_{(n-1)\,\text{times}} w(p)$ where $w \circ w(p) = w^2(p),\ (w \circ w \circ w)(p) = w \circ w^2(p) = w^3(p)$ and so on.

For purposes of exposition, we consider the 2-parameter probability weighting function (pwf) introduced by Prelec (1998, Prop. 1, pg. 503):

$$w(p) = \exp(-\beta(-\ln(p))^{\alpha}),\ 0 < \alpha < 1,\ \ \beta > 0 \tag{2.8}$$

Here α determines the curvature of the pwf. It determines the orientation of the curve. In contrast, β determines the elevation or how much weight is given to a particular curvature.

We refer to (α, β) as a *sentiment pair*. After log differentiation we get

$$\ln[w'(p)] = a(p; \alpha, \beta) = \ln(\alpha\beta) + (\alpha - 1)\ln(-\ln(p)) - \ln(p) - \beta(-\ln(p))^{\alpha} \tag{2.9}$$

Monotonicity of $w(p)$ guarantees that $w'(p) > 0$ so the absolute value requirement in (2.7) is satisfied. However, the true probability weighting function $w(p)$ is unknown, so the parameters α and β are unobservable in psychological phase space.

2.4 Stochastic Lyapunov exponent process in econometrics theory

The stochastic Lyapunov exponent concept was presented in nonlinear time series analysis in the early 1990s via its estimation with nonparametric regressions.[13] Refer to Nychka et al. (1992); McCaffrey et al. (1992) and references therein. Important papers by Bougerol and Picard (1992); Whang and Linton (1999); Shintani and Linton (2004) extended the concept to the econometrics theory literature. Recently, Park and Whang (2012, p. 64) introduced a nonparametric test for random walk against a chaos alternative. In their model the sample estimate for the Lyapunov exponent process of interest is a Brownian functional[14]

$$\lambda_n(t) = \int_0^t \ln|m_n^o(\sqrt{n}B_n(s))|ds, \quad t \in [0, 1] \tag{2.10}$$

where m_n^o is the first derivative of a Nadaraya-Watson kernel estimator for the nonparametric nonlinear function $m_n(\cdot)$, defined on the space of continuous function $C[0, 1]$ on the closed unit interval, endowed with the sup norm metric, and $B_n(t) \in C[0, 1]$ is approximate Brownian motion. Ben Saïda (2012); Ben Saïda (2014) applied the tests above to financial time series that include the S&P 500 index and failed to find chaos in the data. In the sequel, our sample function for the Lyapunov exponent process is also a Brownian functional of $B_n(t)$ but its "kernel estimator" m_n^o is parametric.

[13]In fact, its roots can betraced to the seminal paper by Furstenberg and Kesten (1960).

[14]Refer to Karatzas and Shreve (1991, p. 185) for technical details on this concept.

2.5 Representation theorem for BELLE process

Consider a large sample of N heterogenous decision makers (DMs) at time t. Let $\epsilon_j(t),\ j = 1,\ldots,N$ be the behavioural (or measurement) error associated with the choice made by the j-th investor (DM) at time t. Furthermore, assume that $\epsilon_j(t) \sim iid(0,\sigma^2)$. We assume a common core belief in (2.9) so the model is represented by appending measurement error ϵ_j to (2.9) such that

$$a^j(t,p;\alpha,\beta) = a(p;\alpha,\beta) + \epsilon_j(t) \tag{2.11}$$

$$\ln[w'^j(t,p;\alpha,\beta)] = a^j(p;\alpha,\beta) \tag{2.12}$$

Let $[0,T]$ be the finite time interval for which Lyapunov exponents are observed for each DM. Without loss of generality we normalize the time interval to coincide with $[0,1]$ and let $\Pi^{(n)} = \{0, t_1^{(n)}, t_2^{(n)}, \ldots, t_k^{(n)}, \ldots, 1\}$ partition $[0,1]$ into dyadic intervals such that $t_k^{(n)} = k.2^{-n}$.

Consider the cumulative effect of DMs behavioural errors at time $t \in [t_k^{(n)}, t_{k+1}^{(n)})$ defined by the partial sums S_{nt}^j and $S_{[nt]}^j$ below.[15] Hey (1995) specified an experiment with time dependent behavioural error in stochastic choice so this assumption is admissible. Let

$$S_{nt}^j = \sum_{k=1}^{nt} \epsilon_j(t_k^{(n)}), \qquad S_{[nt]}^j = \sum_{k=1}^{[nt]} \epsilon_j(t_k^{(n)}) \tag{2.13}$$

where $[nt]$ is the integer part of nt. In the psychology and neuroscience literature (2.13) is the basis for a random accumulator model (RAM) of decision making over time. Most

[15] The partial sums allow us to construct an approximate random function as follows. Suppose $\epsilon \sim (0,\sigma^2)$. Divide the interval $[0,1]$ into n equal parts $i/n,\ i = 1,\ldots,n$. Define $S_i = \epsilon_1 + \cdots + \epsilon_n$. Let $W_n(i/n) = \frac{1}{\sigma\sqrt{n}} S_i$. For $t \in [(i-1)/n,\, i/n]$ we interpolate to get

$$W_n(t) = \frac{i/n - t}{1/n} W_n((i-1)/n) + \frac{(t-(i-1)/n)}{1/n} W_n(i/n) = \frac{1}{\sigma\sqrt{n}} S_{i-1} + n\,(t-(i-1)/n)\,\frac{1}{\sigma\sqrt{n}}\epsilon_i$$

For t in the half open interval $[(i-1)/n,\, i/n)$ we have $i-1 = [nt]$. So we get

$$W_n(t) = \frac{1}{\sigma\sqrt{n}} S_{[nt]} + (nt - ([nt])\,\frac{1}{\sigma\sqrt{n}}\epsilon_{[nt]+1}$$

important, RAMs admit "changes of mind" or reversal when the partial sums hit a given threshold (Resulaj et al., 2009). The random broken line connecting the points $([nt], S^j_{[nt]})$ and (nt, S^j_{nt}) is given by

$$W^j_n(t) = S^j_{[nt]} + (nt - [nt])\epsilon_j([nt] + 1) \tag{2.14}$$

By Donsker's Theorem, i.e. functional central limit theorem, we assume $W^j_n(t)$ is an approximate Brownian motion in the space of continuous functions $C[0, 1]$.[16] Let $w(t, p; \alpha, \beta)$ be the state of the core pwf at time t, i.e. continuous in time t, measurable in probability p, and time homogenous in sentiment (α, β). According to Gikhman and Skorokhod (1969, pp. 370-371), by virtue of (2.9), the incremental change in time dependent pwf for the j-th DM at time t can be written as

$$\Delta \ln[w'^j(t; p, \alpha, \beta)] = a^j(p; \alpha, \beta)\Delta t + \sigma \Delta W^j_n(t) \tag{2.15}$$

This paves the way in the limit for the following behavioural empirical local Lyapunov exponent (BELLE) random field

Theorem 2.1 (BELLE random field)**.** *Assume that DMs probabilistic risk attitudes at time t are characterized by Prelec (1998) 2-parameter pwf $w(t, p) = \exp(-\beta(-\ln(p))^\alpha)$. For a given probability measure space $(\Omega, \mathcal{F}, P)$ that satisfies the usual conditions (see e.g. Karatzas and Shreve, 1991), and sample size N of DMs whose preferences are measured with behavioural error $\epsilon_j(t, \omega) \sim$ iid $N(0, 1)$, $j = 1, \ldots, N$ the behavioural stochastic Lyapunov exponent random field $\bar{\lambda}_N(t, p; \alpha, \beta)$ for the sample has the following representation*

$$d\bar{\lambda}_N(t, p, \omega; \alpha, \beta) = \bar{a}_{m,N}(p; \alpha, \beta)dt + \sigma d\overline{W}_{n,N}(t, \omega), \tag{2.16}$$

where $\bar{a}_{m,N}(p; \alpha, \beta)$ is a drift term, σ is a volatility coefficient, and $\overline{W}_{n,N}(t, \omega)$ is an approximate Brownian motion.

Proof. See Appendix B. □

Remark 2.1. The BELLE random field is tangentially related to Park and Whang (2012) Brownian functional result in (2.10). The *existence and uniqueness* (Gikhman and Skorokhod, 1969, Ch. VIII, §3) of $\bar{\lambda}_N(t, p, \omega; \alpha, \beta)$ is implied by Definition 2.1.

[16] This is a common assumption in econometrics theory (White, 2001, Ch. 7) and probability theory (e.g. Serfling (1980, p. 41); Knight (1962); Gikhman and Skorokhod (1969, pp. 452-453); and Karatzas and Shreve (1991, pg. 66)).

*** Insert Figure 7 about here ***

Figure 7 provides estimates of the sample paths for the random field $\bar{\lambda}_N(t, \cdot, \omega; \alpha, \beta)$ over time. It shows that most of the time the market is stable and attains a coffin state. However, there is a maximal state $\sup_{\{0<t<\infty\}} \bar{\lambda}_N(t, \cdot, \omega; \alpha, \beta)$ that explodes in finite time and the market crashes.

*** Insert Figure 8 about here ***

2.5.1 Reranking of credit ratings and market sentiment dynamics

Figure 8 depicts probability dynamics induced by a re-ranking of outcomes. For example, as DMs receive new information about outcomes they may re-rank those outcomes. This re-ranking causes a redistribution of probabilities and the weights given to those probabilities. It is reflected by "spin" around the fix point probability. The BELLE process reflects the local stochastic stability induced by the "spin". As a practical example, credit agencies use information about firms that causes them to rank assets by grade, i.e. AA, Aa, B, etc. This ranking is associated with a probability of default, say. As new information comes in, firms assets are given new ratings that cause a redistribution of probability of default. The extent of probability redistribution dynamics can cause DMs sentiment about firms assets to shift from optimism to pessimism (the case depicted in Figure 8) or *vice versa* with behavioural error. The tail probabilities associated with shifts from optimism to pessimism, for the BELLE process, are estimated next.

2.6 Estimating the probability of transition from stable to unstable state

To estimate the probability of stability, for the BELLE random field, we rewrite $\overline{W}_{n,N}(t)$ in Lemma 1 in Appendix C as an approximate Brownian motion

$$\overline{W}_{n,N}(t) \equiv W_n\Big(\frac{t}{N}\Big), \quad M_{n,N}(t) = \sup_{0\leq s\leq t} \overline{W}_{n,N}(s) \tag{2.17}$$

If $\phi(\cdot)$ is the probability density function for $\overline{W}_{n,N}(t)$, then the probability density function for $M_{n,N}(t)$ is proportional to $\phi(\cdot)$, and $M_{n,N}(t)$ is a Brownian motion (e.g. Gikhman and Skorokhod (1969, pg. 286) and Karatzas and Shreve (1991, pg. 96, Prob. 8.2)).[17] The stochastic stability condition in Lemma 1 in Appendix C is characterized by

$$\begin{aligned}&\Pr\Big\{M_{n,N}(t) < -\frac{1}{\sigma}\bar{a}_{m,N}(p;\alpha,\beta)t\Big\}\\ &= \Pr\Big\{\sup \overline{W}_{n,N}(s) = \sup \frac{\sqrt{t}}{N}\sum_{j=1}^{N} W_n^j(1) < -\frac{1}{\sigma}\bar{a}_{m,N}(p;\alpha,\beta)t\Big\}\end{aligned} \tag{2.18}$$

So the stochastic instability condition is characterized by the complement probability

$$\Pr\Big\{M_{n,N}(t) \geq -\frac{1}{\sigma}\bar{a}_{m,N}(p;\alpha,\beta)t\Big\} = 1 - \Pr\Big\{\sup \frac{1}{N}\sum_{j=1}^{N} W_n^j(1) < -\frac{1}{\sigma}\bar{a}_{m,N}(p;\alpha,\beta)\sqrt{t}\Big\} \tag{2.19}$$

Here, $M_{n,N}(t)$ induces a Lyapunov-Perron effect[18] with tail event large deviation probability of instability given by (2.19) in a seemingly stable system (Leonov and Kuznetsov, 2007, p. 1079).

Theorem 2.2 (Probability of tail event instability for a seemingly stable source function)**.** *Assume that at time t a large sample size N of DMs follow a BELLE random field represented by Theorem 2.1. Then the large deviation probability of tail event stability is given by*

$$\lim_{N\to\infty}\frac{1}{N}\log\Pr\Big\{M_{n,N}(t) \leq -\frac{1}{\sigma}\bar{a}_{m,N}(p;\alpha,\beta)t\Big\} \approx -\frac{\bar{a}^2_{m,\infty}(p;\alpha,\beta)}{2\sigma^2}t$$

Thus, given an initial stable state with probability $\pi_0 = 1$ at time t_0, for stationary transition probability with stable state (s) starting at time t_0, and becoming unstable (u) at time $t+t_0$,

[17] Without loss of generality we assume that the constant of proportionality is 1.

[18] This effect stems from the notion of hyperbolic fixed points and unstable manifolds (Wiggins, 2003, pp. 12, 50). Cursory inspection of Figure 23 and Figure 24 show that $w(P)$ is hyperbolic in a sufficiently large neighbourhood $B_\delta(p^\star)$ of the fixed point $p^\star$. So it contains an invariant manifold in $\mathbb{R}^2$.

in the limit we have

$$\Pr(\text{unstable at } t+t_0 | \text{ stable at } t_0) = P_{us}(t,p) = 1 - \exp\left(-\frac{\bar{a}^2_{m,\infty}(p;\alpha,\beta)}{2\sigma^2}t\right) \tag{2.20}$$

Proof. See Appendix D. □

Remark 2.2. In the sequel we assume stationary transition probabilities. The interested reader is referred to (Dynkin, 1960; Chung, 1960) for more on this concept.

*** Insert Figure 9 about here *** *** Insert Figure 10 about here *** *** Insert Figure 11 about here ***

Cursory inspection of (2.20) shows that given α, β, σ at time t the stationary transition probability of instability $P_{us}(t,p) = 1 - \exp\left(-\frac{\bar{a}^2_{m,\infty}(p;\alpha,\beta)}{2\sigma^2}t\right)$ increases when $\exp(\cdot)$ gets smaller as $\bar{a}^2_{m,N}(p;\alpha,\beta)$ gets larger.[19] These observations are supported by Figure 9 which depicts the almost sure stationary transition probability of instability over time, i.e. $\lim_{t\to\infty} P_{us}(t,p) \to 1$.[20] The cross-sectional plots in Figure 10 show that for time normalized in $[0,1]$, over small time window $2\Delta t = 2/T = 2/156 \approx 0.01$, the tail event probability of a stable market becoming unstable, i.e. $P_{us}(t,p)$, is almost zero in the range depicted on the vertical axis across probability ranks. As the time window gets larger, i.e. $144\Delta t$, the range for probability of market instability narrows to $P_{us}(t,p) \in [.985, 1.0]$. In Figure 11 the probability of instability $P_{us}(t,p)$ takes a long time for the BELLE drift $\overline{a}(p;\alpha,\beta)$ across all probability ranks.

2.7 Drift term characterization of BELLE process

To evaluate the impact of the other control variables on Lyapunov-Perron type probability of instability we turn to comparative statics. Rewrite the drift term in Theorem 2.1 for given p so that

[19] The same also holds for fixed m and increasing t.

[20] In order not to overload the paper we did not include analytics for a two state $((u,v)$ Markov transition probability matrix.

$$f(\alpha,\beta;p) = \ln(\alpha\beta) + (\alpha-1)\ln(-\ln(p)) - \ln(p) - \beta(-\ln(p))^{\alpha} \tag{2.21}$$

$$\frac{\partial f}{\partial \alpha} = \alpha^{-1} + \ln(-\ln(p)) - \beta(-\ln(p))^{\alpha+1} \tag{2.22}$$

$$\frac{\partial f}{\partial \alpha} > 0 \Rightarrow 0 < \beta < \frac{\frac{1}{\alpha} + \ln(-\ln(p))}{(-\ln(p))^{\alpha+1}} \tag{2.23}$$

Similarly,

$$\frac{\partial f}{\partial \beta} = \frac{1}{\beta} - (-\ln(p))^{\alpha}, \quad \frac{\partial f}{\partial \beta} > 0 \Rightarrow 0 < \beta < (-\ln(p))^{-\alpha}, \quad \frac{\partial^2 f}{\partial \beta \partial \alpha} = -(-\ln(p))^{\alpha+1} \tag{2.24}$$

The first order effects for increasing drift (and hence increased probability of instability) in (2.23) and (2.24) is given by

$$0 < \beta < \max\left\{\frac{\alpha^{-1} + \ln(-\ln(p))}{(-\ln(p))^{\alpha+1}}, \ \ (-\ln(p))^{-\alpha}\right\} \tag{2.25}$$

Note that $\partial^2 f/\partial\beta\partial\alpha$ shows that α and β are independent (Gonzalez and Wu, 1999, p. 139) Since α controls the curvature of $w(p)$, it determines the degree of DM's sentiment. Whereas β is an elevation parameter that controls (1) the location of fixed point probability in the underlying probability distribution, and (2) degree of "cautiously hopeful" behaviour (Lopes, 1995, p. 187). So (2.25) depicts the range of elevation that control the hyperbolic fixed points for invariant manifolds that support stability and instability.[21] In the case of Prelec (1998) single factor model, i.e. $\beta = 1, 0 < \alpha < 1$, we find that the set of feasible values in (2.25) for curvature α are solutions to the nonlinear equation

$$\frac{\alpha^{-1} + \ln(-\ln(p))}{(-\ln(p))^{\alpha+1}} > 1 \tag{2.26}$$

$$\Rightarrow (-\ln(p))^{\alpha+1} - \alpha^{-1} - \ln(-\ln(p)) < 0 \tag{2.27}$$

We summarize the results above in

[21] Refer to Chicone (1999, p. 28) and Wiggins (2003, Ch. 3) for details on hyperbolic fixed points. Chen and Xuefeng (2003, p. 423) used a similar analytic apparatus to identify conditions for dynamics in their model.

Proposition 1 (Critical values of probabilistic risk factors)**.** *Given a large sample N of DMs with core Prelec (1998) 2-parameter pwfs (α and β) in a behavioral dynamical system with the BELLE process in psychological space in Theorem 2.1, the tail event probability of instability in Theorem 2.2 depends on either of the following*

1. *growth in sample size N or time t or both;*
2. *curvature (α) and elevation (β) of pwfs that induce the range of critical probabilistic risk attitude factors*

$$0 < \beta(p|\alpha) < \max\{\varphi_1(\alpha, p), \varphi_2(\alpha, p)\};$$

3. *increased precision in the diffusion coefficient σ for classifying measurement error or behavioural noise by DMs;*

where $\varphi_1(\alpha, p) = \dfrac{\alpha^{-1} + \ln(-\ln(p))}{(-\ln(p))^{\alpha+1}}$ *and* $\varphi_2(\alpha, p) = (-\ln(p))^{-\alpha}$. □

Remark 2.3. Gonzalez and Wu (1999) show that α and β are independent. Here $\beta(p|\alpha)$ is based on comparative statics. In the sequel we write $\beta(p)$. Budescu et al. (2011) also provide a taxonomy of scenarios where elevation (β) and curvature (α) parameters affect "probability reversals" if DMs weight probabilities that are close together at a different rate. The methodology developed here is distinguished. Here, we show how the elevation and curvature parameters interact to reverse the shape of the entire pwf by rotating the entire pwf about a fixed point.

*** Insert Figure 12 about here ***

3 Market instability identified by BELLE process

In this section we plot and describe the source functions, i.e. pwfs, implied by option prices from parameter estimates in Polkovnichenko and Zhao (2013). We calibrate analytic expressions from our criterion function for market instability in Proposition 1, and compare the predictions of the theory to historic events in option price behavior. The following definition

*** Insert Figure 13 about here ***

*** Insert Figure 14 about here ***

*** Insert Figure 15 about here ***

*** Insert Figure 16 about here ***

is adapted from Wakker (2010, p. 320) and it plays a key role below.

Definition 3.1 (Source function)**.** Assume that all uncertainties can be quantified in terms of probabilities, and that a source is a specific set of events. For each event E define $W(E)$ as $w_{\$}(P_{\$}(E))$ where \$ is the source from which E obtains, $P_{\$}$ is a probability measure on \$, and $w_{\$}$ is the pwf corresponding to E. We call $w_{\$}$ a *source function.* □

3.1 Calibrating source functions implied by S&P 500 index option prices

Polkovnichenko and Zhao (2013, pg. 595, Fig. 9) derived estimates of Prelec (1998) 2-parameter pwf for shape parameter α and elevation parameter β assuming CRRA utility $u(x) = \dfrac{x^{1-\gamma}}{1-\gamma}$ and $\gamma = 0, 1, 2$, for $S\&P500$ index option price data for, among others, 28-days maturity over the sample period January 1996 to December 2008. So the source functions are term structures for probability ranks. In the sequel we use data for (α, β) collected by eyeballing Polkovnichenko and Zhao (2013, Fig. 6) for risk neutral CRRA index $\gamma = 0$, and risk averse CRRA index $\gamma = 2$. For $\gamma = 0$, the burden of risk attitudes is carried entirely by the source function (Yaari, 1987). For $\gamma = 2$, the burden is shared: risk aversion carried mostly by the utility function, and risk seeking is carried by the source function. Recall that α reflects a DM's discrimination among bets, and β reflects a DM's level of attraction to the bets.

On June 19, 1997 there was pessimism in the options market depicted by the concave-convex inverted S-shape curve ($\alpha = 0.56$, $\beta = 0.93; \gamma = 2$) in Figure 13. This was around the time of the Asian currency crisis (Mishkin, 1999; Corsetti et al., 1999)–depicted in Figure 12 where the VIX spiked in that year. So we label that *credit risk source function* $W^{\text{Asia}}_{\text{currency}} = w^{\text{Asia}}_{1997}(p;\, \alpha = 0.56,\, \beta = 0.93)$.

By April 21, 2005 the state in the options market changed to optimism depicted by the convex-concave skewed S-shape curve ($\alpha = 1.6$, $\beta = 1; \gamma = 2$) in Figure 13. This time there was a real estate bubble in the US (Zhou and Sornette, 2006) driven by sub-prime loans and asset securitization.[22] This is depicted in Figure 12 where the VIX is

[22] Adelson (2013) argues that sub prime loans and mortgages "may have served as the spark that ignited the

below its 12-month rolling average in 2005. So we label that *credit risk source function* $W^{\text{US}}_{\text{RealEstateCDO}} = w^{\text{US}}_{2005}(p;\, \alpha = 1.6,\, \beta = 1.0)$.

3.1.1 Early warning critical values of probabilistic risk factors for toxic assets

Undeniably, option market sentiment had a *phase transition from pessimism to optimism* between 1997 and 2005, i.e. the underlying pwf flipped based on the source of risk. The $\beta(p)$-instability distribution predicted by Proposition 1 is plotted in Figure 14 for $\beta(p) = \min\{\max\{\varphi_1(\alpha, p), \varphi_2(\alpha, p)\}, \beta_c\}$ where $\varphi_1(\alpha, p) = \dfrac{\alpha^{-1} + \ln(-\ln(p))}{(-\ln(p))^{\alpha+1}}$ and $\varphi_2(\alpha, p) = (-\ln(p))^{-\alpha}$ and β_c is the observed pwf elevation parameter, i.e. the β parameter estimated by Polkovnichenko and Zhao (2013) for $W^{\text{Asia}}_{\text{currency}}$ and $W^{\text{US}}_{\text{RealEstateCDO}}$. A quadratic curve in p was fitted for $\beta(p)$ as indicated. According to Figure 14, the region of instability for both curves in Figure 13 is supported by probability values less than the fixed point probability $p^* = 0.4$. For example, $0 < p \leq 0.4$ for $W^{\text{Asia}}_{\text{currency}}$ and $W^{\text{US}}_{\text{RealEstateCDO}}$. This is the probability support for low ranked index option prices. It reflects low ranked assets. Figure 14 shows that DMs with $\alpha = 1.6$ and $0.26 \leq \beta(p) < 0.74$ are prone to induce instability in states of optimism or overconfidence when $\beta_c = 1$. In contrast, DMs with $\alpha = 0.56$ and $0.63 \leq \beta(p) < 0.93$ are prone to induce instability in states of pessimism or underconfidence when the true $\beta_c = 0.93$. According to Polkovnichenko and Zhao (2013, p. 585) β shifts the distribution and α mainly affects the tails.

powder keg" of underlying causes of the Great Recession of 2008 but it was not the cause. The Financial Crisis Inquiry Comission (2011, Ch. 10) referred to this period as "The Madness".

Table 1: Parameter values for credit risk source functions

Parameter	Asia 1997 Currency Crisis	US 2005 Real Estate & CDO Bubble
α-curvature	0.56	1.60
β-elevation	0.93	1.00
$p^{\star}$-fixed point	0.40	0.40
$\beta(p)$-instability	0.60	0.20
	0.70	0.50
$\beta(p)$-tipping point	0.93	0.67

The plots corresponding to the parameter values above are depicted in Figure 13, Figure 14, Figure 15 and Figure 16. Tipping point values for $\beta(p^{\star})$ are depicted in Figure 14.

3.2 Calibrating source functions predicted by critical values of market instability criteria

In the analysis that follows we reiterate that pwfs are identified with the source of credit risk so they are source functions in accord with Definition 3.1. Table 1 presents parameter values used in the analysis below.

3.2.1 Source function for US real estate and CDO bubble circa 2005

To illustrate our theory for US real estate and CDO source functions, we select $\beta(p)$-instability values $\beta = 0.25$ and $\beta = 0.5$ from the distribution of critical values predicted by Proposition 1 to characterize dynamics of the underlying source functions. The orientation of the skew S-shaped source function $W^{\text{US}}_{\text{RealEstateCDO}}$ for $(\alpha = 1.6, \beta = 1.0; \gamma = 2)$ in Figure 13 switched to an all concave shape in Figure 15 depicting *ex ante* $W^{\text{US, crash}}_{\text{RealEstateCDO}}(p; crit(\alpha = 1.6, \beta = 0.2))$ for fixed $\alpha = 1.6$, and critical value $\beta = 0.2$. So the relative strength of DMs confidence is such that they are now uniformly fearful and pessimistic over the entire range of rank ordered option prices. Similarly, in Figure 16 the *ex ante* source function $W^{\text{US, crash}}_{\text{RealEstateCDO}}(p; crit(\alpha = 1.6, \beta = 0.5))$ is concave for $\alpha = 1.6$ and critical value $\beta = 0.5$. Cursory inspection of Figure 15 and Figure 16 show $W^{\text{US, crash}}_{\text{RealEstateCDO}}(p; crit(\alpha = 1.6, \beta = 0.2)) > W^{\text{US, crash}}_{\text{RealEstateCDO}}(p; crit(\alpha = 1.6, \beta = 0.5))$. According to Hogarth and Einhorn (1990, Fig. 2, Fig. 4, pp. 786-787) the higher curve implies greater ambiguity in the market. In this case it depicts more pessimism (Gonzalez and Wu, 1999, p. 138) about toxic assets, and each of those functions symbolize eminent market crash.

3.2.2 Source function for Asian currency crisis circa 1997

The elevation of the inverse S-shaped source function $W_{1997}^{\text{Asia}}(p;\, \alpha = 0.56,\, \beta = 0.93)$ in Figure 13 for $\alpha = 0.56, \beta = 0.93; \gamma = 2$ has a fixed point probability $p^* = 0.4$. However, when $\beta = 0.6$ the fixed point probability jumped from 0.4 to about $p^* = 0.75$ in Figure 15. According to Hogarth and Einhorn (1990, Fig. 2, pp. 785-786), this northeast movement of the fixed point from $p^* = 0.4$ to $p^* = 0.75$, associated with *ex ante* source function $W_{1997}^{\text{Asia}}(p;\, crit(\alpha = 0.56,\, \beta = 0.6))$, implies larger anticipated losses. In this case the market was more cautious than hopeful. In contrast, when $\alpha = 0.56$ and $\beta = 0.7$ the fixed point probability for *ex ante* source function $W_{1997}^{\text{Asia}}(p;\, crit(\alpha = 0.56,\, \beta = 0.7))$ falls to about $p^* = 0.7$ in Figure 16. In this case, the market was less cautious and more hopeful compared to when $p^* = 0.75$. Each one of the source function plots in Figure 15 and Figure 16 depict probabilistic preference reversal relative to the corresponding plots in Figure 13. Evidently, $\beta(p)$ attractiveness levels shifts the underlying distribution for given sentiment reflected by α discrimination among bets on index option prices.

*** Insert Figure 17 about here ***

3.3 Snap shots of source function dynamics that predict market crash

In this section we examine snap shots of market dynamics that signal eminent market crash. We conduct a natural experiment with the source functions implied by S&P 50 index option prices when CRRA $\gamma = 0$. In that way, all market sentiments and risk attitudes are carried by the source functions. Figure 17 depicts the time varying (α_t, β_t) market sentiment pair. Recall that the curvature parameter α reflects discriminating between optimism and pessimism, while β reflects attractiveness among underlying bets (cf. Gonzalez and Wu, 1999). The plot shows that discrimination among index option prices vary widely while their attractiveness remains comparatively stable in a given range. The critical $\beta(t,p)$ plot predicted by the BELLE process shows a lot more variability over time. This reflects the notion that the market switches from stable to unstable states over time depending on the attractiveness of bets in the index option market.

*** Insert Figure 18 and Figure 19 about here ***

Figure 20 provides external validation for the market crash scenarios represented by our source function analysis. It depicts 5th-degree polynomial smoothers for weekly

*** Insert Figure 20 about here ***

sentiment data for Bulls, Bears, and Risk Neutral survey participants for American Association of Individual Investors data for the period June 1987 to December 2018. During the Great Recession of 2008, triggered in part by the US Real Estate market failure, there was very little difference of opinion between Bulls and Bears. In fact, the Bears were slightly more bullish than the Bulls! Similarly, during the 1990 Japanese Real estate crisis (Peek and Rosengren, 2000) there was no difference of opinion between Bulls and Bears and markets crashed. Figure 20 shows that when markets crash bull and bear sentiments coincide. So we would expect a small volume of trade or no trade at all, because the market breaks down since all traders hold the same beliefs about asset quality (e.g. Akerlof (1970); Harris and Raviv (1993) and Stiglitz and Grossman (1976, p. 250)).

*** Insert Figure 21 about here ***

Figure 21 provides monthly snap shots of market dynamics leading up to the Lehman Brothers bankruptcy filing in September 2008–the largest in history–and markets crashed. However, our BELLE process signalled eminent market crash at least 2-months before in July 2008 as shown by the limit tent map shape for source functions. In October 2008, one month after the crash, investors began the process of reversing likelihood insensitivity. By November, investors exhibit even less likelihood insensitivity in that they no longer treat market events as impossible. In December 2008, some investors resorted to treating market events as impossible but others were able to discriminate among assets.

4 Conclusion

We contribute to the literature on investor psychology, financial market surveillance, and financial market (in)stability by constructing a behavioural random field (BELLE) from investors sentiment about probability ranks, and applied it in a natural experiment with index option prices. We show how the shape of probability weighting functions (pwfs) implied by index option prices depend on the prevailing sources of risk in the market so they are "source functions".

While our model cannot predict the precise date of a market crash, it predicts critical out-of-sample tipping point values. For a single output parameter, and given market sentiment input parameter(s), it predict market crash signals. We illustrated the model's robustness across different risk sources. Furthermore, we provide snap shots of monthly market dynamics generated by the BELLE process which would have predicted the Great Recession of 2008. One of the surprising results produced by the BELLE process is the limit tent map shape of source functions before market crash. To the best of our knowledge, this paper is the first to establish a connection between probabilistic risk attitudes in financial markets and limiting tent map shapes popularized in the literature on nonlinear dynamics in financial markets. Thus, we provide new tools for identifying early warning signals for market instability.

We also provide closed form solutions for time dependent transition probability that a seemingly stable financial market will become unstable. In fact, model simulation produces the rather fatalistic result that financial market crashes are inevitable in finite time as long as they are driven by investors' sentiment. It is left to be seen whether the transition probability relationship can be extended to stochastic volatility in the BELLE process.

5 APPENDIX

A Proof of invariant manifold Proposition 2

In nonlinear dynamics the stable manifold theorem (stated in Appendix G.1.2) plays a key role in identifying stable and unstable fixed points. It essentially decomposes an invariant manifold into stable and unstable components (Chicone, 1999, Ch. 4). Here we apply the stable manifold theorem in the context of pwfs.

Proposition 2 (Invariant manifold for probability weighting functions)**.** *Let F be a cumulative probability distribution, and $w(F)$ be a probability weighting functional. Define the set*

$$C(F) = \{F| - w(F)\ln(w(F)) = F,\ 0 \leq F \leq 1\} \tag{A.1}$$

Then $C(F)$ is an invariant set of fixed point functions for probability weighting. Moreover, in the restricted case when $w(F) = F$ we get $C(F) = \{0,\ e^{-1},\ 1\}$ where $F = p^\star = e^{-1}$.

Remark A.1. McLennan (2018, Fig. 1.2) identified sets like $C(F)$ as an *essential set* of fixed points. Alternatively, $C(F)$ is an invariant subspace of $[0, 1]$. That is, $w : C(F) \to C(F) \subset [0, 1]$ and $C(F)$ is an invariant manifold.

Proof. By construction we can rewrite $w(F) = \exp(-\frac{F}{w(F)})$. The distribution function(s) F which solves that nonlinear equation represents fixed probability distributions that satisfy the equation. By definition, F represents a continuum of probabilities. Specifically,

1. let ξ_p be the p-quantile of F. Define the set of probabilities $X(p) = \{p| - w(p)\ln(w(p)) = p,\ F(\xi_p) = P(X \leq \xi_p) = p,\ F \in C(F)\}$. By construction $X(p)$ is a cluster set of probabilities since it contains the accumulation or fixed points p that satisfy the entropy equation, and by construction $X(p) \subseteq C(F)$. Hence $C(F)$ is a hereditary cluster set.

2. Suppose $F \in C(F)$, and $p \notin X(p)$. The latter relation implies that $-w(F(\xi_p))\ln(w(F(\xi_p))) \neq F(\xi_p)$ and $F(\xi_p) \notin C(F)$. This contradicts our incipient hypothesis $F \in C(F)$. In which case $F(\xi_p) = p \in X(p)$ and $C(F) \subseteq X(p)$.

The results of 1. and 2. imply that $C(F) = X(p)$. In which case $C(F)$ is a cluster set of probabilities. The restriction $W(F(\xi_p)) = F(\xi_p) = p$ produces the fixed point solution $W(F) = F = \exp(-1)$. □

Corollary 1 (Invariant manifold decomposition)**.** *$C(F)$ is decomposable into stable (S) and unstable (U) submanifolds such that $U \oplus S = C(F)$.*

Proof. Apply the stable manifold theorem in Appendix G.1 to $C(F)$ in Proposition 2. □

Remark A.2. Since w is defined on $C(F)$ the invariance decomposition property implies $w(S(F)) \subset S(F)$ and $w(U(F)) \subset U(F)$. Refer to Appendix G.1 for further details. □

B Proof of representation theorem for behavioural Lyapunov exponent random field Theorem 2.1

Proof. By hypothesis, $\mathcal{F}$ is the σ-field of Borel measurable subsets of the sample space Ω. So our analysis takes place in an open ball or disk $B_\delta(p^\star)$ that support the measurement error $\epsilon(t,\omega)$ for $\omega \in \Omega$. Recall that $a(p;\alpha,\beta) = \ln(\alpha\beta) + (\alpha-1)\ln(-\ln(p)) - \ln(p) - \beta(-\ln(p))^\alpha$ and that $a^j(t,p;\alpha,\beta) = a(p;\alpha,\beta) + \epsilon_j(t,\omega)$. The aggregate change in pwf for heterogeneous DMs in the sample size N is given by

$$\sum_{j=1}^{N} \Delta \ln[w'^j(t,p;\alpha,\beta)] = \sum_{j=1}^{N} a(p;\alpha,\beta)\Delta t + \sigma \sum_{j=1}^{N} \Delta W_n^j(t,\omega) \tag{B.1}$$

Substituting $\Delta \ln[w'^j(t;p,\alpha,\beta)]$ for $\ln|w'(p_j)|$ in (2.7), and by virtue of the continuous mapping theorem (White, 2001, Thm. 7.20, p. 178) replacing Δt and ΔW_n with dt and dW_n, respectively, we get in the limit[23]

$$\frac{1}{m}\sum_{j=1}^{N}\sum_{r=1}^{m} d\lambda^j(t;p,\alpha,\beta) = \frac{1}{m}\sum_{j=1}^{N}\sum_{r=1}^{m} a(p_r;\alpha,\beta)dt + \frac{1}{m}\sum_{j=1}^{N}\sum_{r=1}^{m} dW_n^j(t,\omega) \tag{B.2}$$

Dividing left hand side (LHS) and right hand side (RHS) by N and using "bar" to represent sample average, for a discretized probability distribution $p = (p_1, p_2, \ldots, p_m)$, $\sum_{j=1}^{m} p_r = 1$, we get the behavioural Lyapunov exponent random field

$$d\bar{\lambda}_N(t,p,\omega;\alpha,\beta) = \bar{a}_{m,N}(p;\alpha,\beta)dt + \sigma d\overline{W}_{n,N}(t,\omega), \tag{B.3}$$

$$\bar{\lambda}_N(\cdot) = \frac{1}{N}\sum_{j=1}^{N}\lambda^j(\cdot), \quad \bar{a}_{m,N}(\cdot) = \frac{1}{N}\frac{1}{m}\sum_{j=1}^{N}\sum_{r=1}^{m} a^j(p_r;\alpha,\beta), \quad \overline{W}_{n,N}(t,\omega) = \frac{1}{N}\sum_{j=1}^{N} W_n^j(t,\omega) \tag{B.4}$$

□

C Stochastic stability condition for source functions and option traders' sentiment

Definition C.1 (Stochastic stability)**.** (Gihman and Skorohod, 1972, p. 145). A stationary point $p^\star$ will be called stable if for any $\epsilon > 0$, there exist $\delta > 0$ such that for $B_\delta(p^\star) = \{p : |p - p^\star| < \delta\}$

$$\Pr\{\lim_{t\to\infty} \xi_p(t) = p^\star | \, \xi_p(t) \in B_\delta(p^\star)\} \geq 1 - \epsilon \tag{C.1}$$

where $\xi_p(t)$ is a process (possibly stochastic) starting at p. □

Remark C.1. In our model, the fixed point probability $p^\star$ is a stationary point. (C.1) im-

[23]There is no p_r term on the LHS by definition.

ply that initial values for $\xi_p(t)$ converge uniformly to $p^\star$ over time (Arnold, 1984, p. 210). Specifically, $B_\delta(p^\star)$ is a basin of attraction of $p^\star$ and $p^\star$ is Lyapunov stable (e.g. Medio and Lines, 2003, pp. 67-68). $\square$

After integrating the stochastic differential equation in Theorem 2.1 we get the behavioural Brownian functional

$$\bar{\lambda}_N(t; p, \alpha, \beta) = \int_0^t \bar{a}_{m,N}(p; \alpha, \beta) du + \sigma \int_0^t d\overline{W}_{n,N}(u) \tag{C.2}$$

$$= \bar{a}_{m,N}(p; \alpha, \beta)t + \sigma\big(\overline{W}_{n,N}(t) - \overline{W}_{n,N}(0)\big) \tag{C.3}$$

Recall that $M_{n,N}(t) = \sup_{0\leq s\leq t} \overline{W}_{n,N}(t)$. The stochastic Lyapunov exponent stability condition implies that the exponent is negative (e.g. (Leonov and Kuznetsov, 2007; Hommes and Manzan, 2006), and Wiggins (2003, p. 7)) and it is given by the folowing

Lemma 1 (Stochastic Lyapunov exponent stability condition)**.** *The BELLE process is stable when*

$$\sup_t \bar{\lambda}_N(t; p, \alpha, \beta) < 0 \implies M_{n,N}(t) < \overline{W}_{n,N}(0) - \frac{1}{\sigma}\bar{a}_{m,N}(p; \alpha, \beta)t \tag{C.4}$$

$$\implies M_{n,N}(t) < -\frac{1}{\sigma}\bar{a}_{m,N}(p; \alpha, \beta)t \tag{C.5}$$

where $\overline{W}_{n,N}(0) = 0$*, and* $M_{n,N}(t)$ *is a Brownian motion.* $\square$

Thus, in the context of Definition C.1 the stochastic stability condition for pwfs is characterized by (C.5).

D Proof of Large Deviation Theorem 2.2 for transition from stable to unstable market states

Proof. By hypothesis, $M_{n,N}(t) = \sup_{0\leq s\leq t} \overline{W}_{n,N}(s)$. So, $M_{n,N}(t)$ is also a Brownian motion (e.g. Gikhman and Skorokhod (1969, pg. 286) and Karatzas and Shreve (1991, pg. 96, Prob. 8.2)). According to the Cramer-Chernoff Theorem (Olivieri and Vares, 2005, Thm 1.1, pp. 5-6), given a sequence of iid random variables $(X_1, X_2, \ldots, X_n)$ with mean 0, and variance 1, $S_n = \sum_{i=1}^n X_i$ and sample mean $\bar{X}_n = S_n/n$, with moment generating function is $M(\theta) = E[\exp(\theta X)]$ and rate function $I_\mu(x) = \sup_{\theta\in\mathbb{R}} (\theta x - \log M(\theta))$, the large deviation probability for lower bounds is given by

$$\liminf_{n\to\infty} \frac{1}{n} \log \Pr\left\{\bar{X}_n \leq x\right\} \geq -I_\mu(x) \tag{D.1}$$

Since $M_{n,N}(t)$ is a Brownian motion, it is normally distributed with mean 0, and variance t. So the moment generating function is of type $M(\theta) = \exp(\frac{t\theta^2}{2})$. $I_\mu(x)$ attains its maximum when $x = \theta t = \arg\max_{\theta} \left(\theta x - \frac{t\theta^2}{2}\right)$, i.e. $I_{\mu}^{\max} = t\theta^2/2$. However, of interest to us in (2.19) is

$$M_{n,N}(t) = \sup_{0 \le s \le t} \overline{W}_{n,N}(s) < -\frac{\bar{a}_{m,N}(p; \alpha, \beta)}{\sigma} t \tag{D.2}$$

By virtue of (B.4) and the scaling property of Brownian motion (Karatzas and Shreve, 1991, p. 104), $\overline{W}_{n,N}(t) = \frac{\sqrt{t}}{N} \sum_{j=1}^{N} W_n^j(1)$. So, we rewrite an equivalent probability statement

$$\Pr\left\{\sup_{0 \le s \le t} \overline{W}_{n,N}(s) < -\frac{\bar{a}_{m,N}(p; \alpha, \beta)}{\sigma} t\right\} \tag{D.3}$$

Thus, the effective x from (D.3) for substitution in the rate function in (D.1) is $x_{\text{eff}} = \theta_{\text{eff}} = -\frac{\bar{a}_{m,N}(p;\alpha,\beta)\sqrt{t}}{\sigma}$ and $I_{\mu}^{\max} = \theta_{\text{eff}}^2 = \frac{\bar{a}_{m,N}^2(p;\alpha,\beta)t}{2\sigma^2}$. By virtue of the Cramer-Chernoff bound in (D.1), (2.18) and θ_{eff} we get the large deviation probability for being in a stable state

$$\liminf_{N \to \infty} \frac{1}{N} \log \Pr\left\{M_{n,N}(t) = \sup_{0 \le s \le t} \overline{W}_{n,N}(s) \le x_{\text{eff}}\right\} \ge -I_{\mu}(x) = -\frac{\bar{a}_{m,\infty}^2(p; \alpha, \beta)}{2\sigma^2} t \tag{D.4}$$

Assuming an initial stable state with probability $\pi_0 = 1$ at time t_0, and stationary transition probability, as $N \to \infty$ we get the large deviation conditional probability of being in an unstable state as the complement of (D.3) or (D.4)

$$\mathit{Pr(unstable\ at\ } t + t_0 \mathit{|\ stable\ at\ } t_0\mathit{)} = P_{us}(t, p) = 1 - \exp\left(-\frac{\bar{a}_{m,\infty}^2(p; \alpha, \beta)}{2\sigma^2} t\right) \tag{D.5}$$

□

E The Polkovnichenko-Zhao estimator for Prelec's 2-factor pwf

The probability weighting function in Polkovnichenko and Zhao (2013) was estimated as follows. Further details are in their paper. Let

$$w(P_0) = c\left[\frac{Q(R_0)}{u'(R_0)} + \int_0^{R_0} Q(R) \frac{u''(R)}{u'(R)^2} dR\right] \tag{E.1}$$

where

$$w(P) = \exp\left(-(-\ln(P^{\beta}))^{\alpha}\right), \quad Z(P) = w'(P), \quad u(R) = R^{1-\gamma}/(1-\gamma) \tag{E.2}$$

$$c = \left(\int_0^{\infty} \left(q(R)/u'(R)\right) dR\right)^{-1}, \quad q(R) = \frac{R^{-a} Z(P) p}{E[R^{-\gamma} Z(P)]} \tag{E.3}$$

where P is a cdf and p is the corresponding pdf, and Q is the distribution function for q, and R is gross return on investor wealth W. For specific P_0 with corresponding R_0 we have $P(R_0) = P_0$. In general, $Z(P)$ was estimated nonparametrically in a first stage by signal extraction from

$$E[m(R^k - R^0)] = 0, \quad m = u'(W)Z(P)$$

for $k = 0, 1, \ldots, N$ assets in a portfolio with wealth W invested in it. $Z(P)$ is extracted by specifying *several different utility functions* for $u(\bullet)$ (Polkovnichenko and Zhao, 2013, p. 588). In a second stage, $w'(P)$ for Prelec (1998) 2-parameters pwf was fitted to get estimates for α, β. The **probabilistic risk attitude factors** α curvature (discriminating among probabilities associates with securities), and β elevation (attractiveness of bet on securities) characterize $w(P)$ (Gonzalez and Wu, 1999).

F Figures

Tail weights for P-ranks: Pessimists vs. Optimists–S&P 500 index option

Figure 3: Likelihood insensitivity over P-ranks

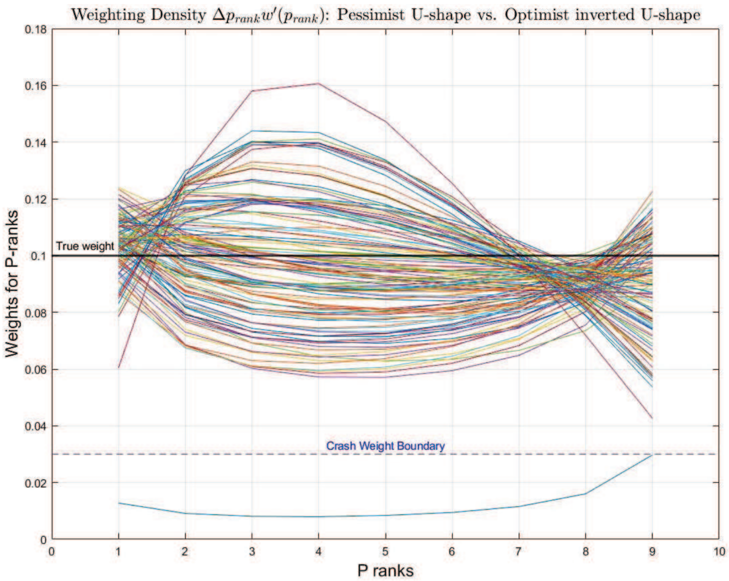

Figure 4: Likelihood insensitivity over time

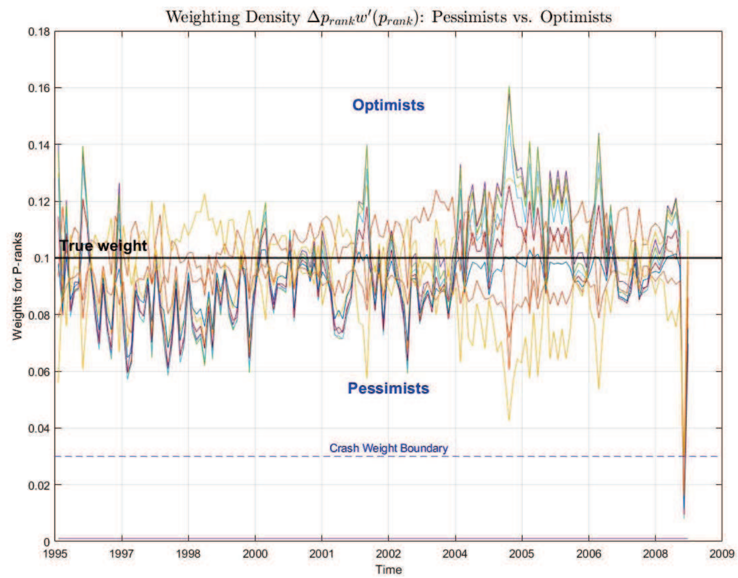

According to bounded subadditivity arguments in Tversky and Wakker (1995, p. 1260), the weighting density (plotted separately over space and time above) induced by subadditivity is $w(P + \Delta P) - w(P) \approx w'(P)\Delta P$ (we suppress the t in $w(t, P)$). Here, $\Delta P = 0.1$ is the "True Weight" increment, and $w'(P) = 1$ represents the slope of the diagonal $w(P) = P$ for linear probability. $w'(P) > 1$ for small probabilities in the *concave-convex* pwf that connotes overweighting small probabilities. This is pessimism. So, the weighting density $w'(P)\Delta P > \Delta P = 0.1$ at low ranks. *Likelihood insensitivity for mid-ranks* implies $w'(P) < 1$. So, $w'(P)\Delta P < 0.1$ and we have a dip below 0.1 as seen in the plots. However, *at high P-ranks*, i.e., $P > 0.9$, we have $w'(P) > 1$ again–this time approaching the diagonal from below. So, it *underweights the probability of high ranks*. And $w'(P)\Delta P > 0.1$. What we just described is the locus of the U-shaped pattern or smile that characterizes pessimists. Note that the opposite slope patterns are observed for optimists, and this generates an inverted U-shaped pattern or frown. Thus, the plot is interpreted as follows:

U-shape pattern: Pessimists overweigh probabilities for low ranks and underweigh probabilities for high ranks. This is a probability smile.

Inverted U-shape: Optimists underweight probabilities for low ranks and overweigh probabilities for high ranks. This is a probability frown.

Crash weight The estimated crash weight boundary is given by $w(P+\Delta P)-w(P) \approx 0.03$. So, there is almost no likelihood insensitivity, i.e. the middle portion of the pwf is flat. This is captured by the line below the crash weight boundary in Figure 3 and the dip below same in Figure 4 above.

Stable and unstable fix points for source functions in index option market

Figure 5: Stable source function fixed points

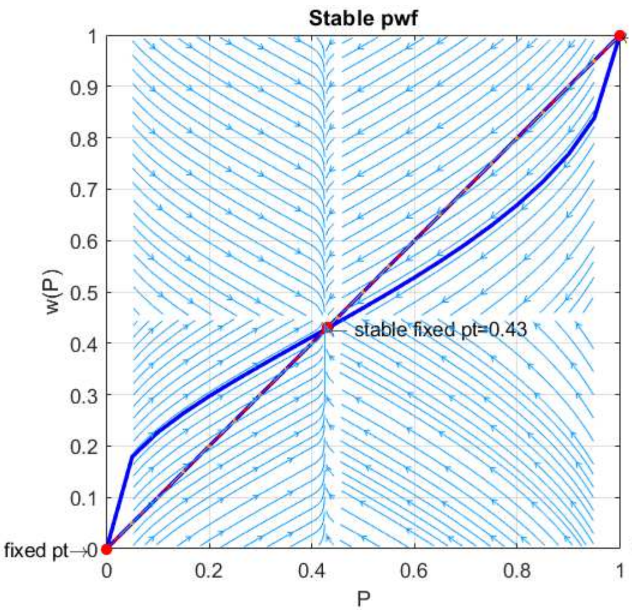

Figure 6: Unstable source function fixed points

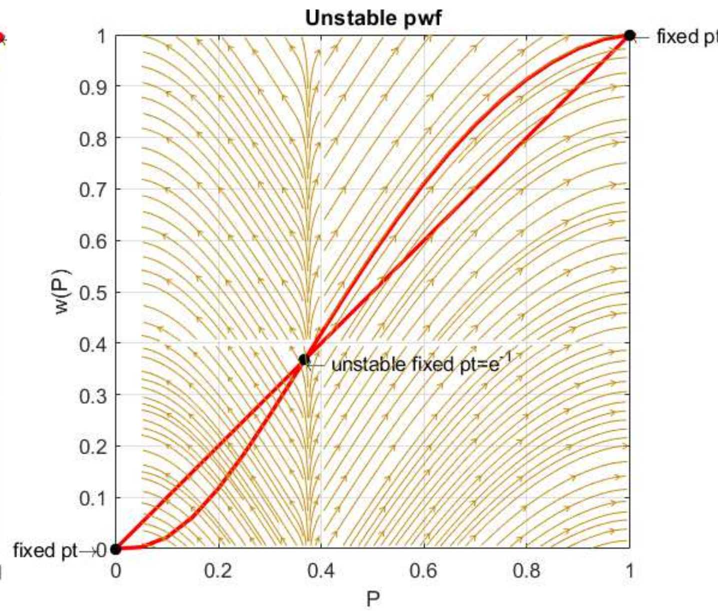

Figure 5 depicts stable fixed points for Prelec's 2-factor pwf calibrated to $\alpha = 0.56, \beta = 0.93$ for monthly index option prices data for 1996-2008 in Polkovnichenko and Zhao (2013). The orbit generated by the iterated functions $p, w(p), w(w(p)), \ldots, w^n(p)$ for that plot converges to the fixed point probability $p = 0.43$ (cf. Prelec, 1998, p. 506). This is a stable attractor because all starting points for the isoclines converge to $p^\star = 0.43$ which is close to $p^\star = e^{-1} \approx 0.37$. It is an empirical realization of the phase portrait in Figure 23. By contrast, Figure 6 depicts an unstable fixed point for $\alpha = 1.6, \beta = 1$. This is an unstable attractor because all the isoclines diverge from $p^\star = e^{-1}$. This is an empirical realization of the phase portrait in Figure 24. Thus, iterative pwf dynamics is dispositive of pwf [in]stability.

BELLE sample paths with coffin states and explosion

Figure 7: BELLE process sample paths with coffin states
and market implosion

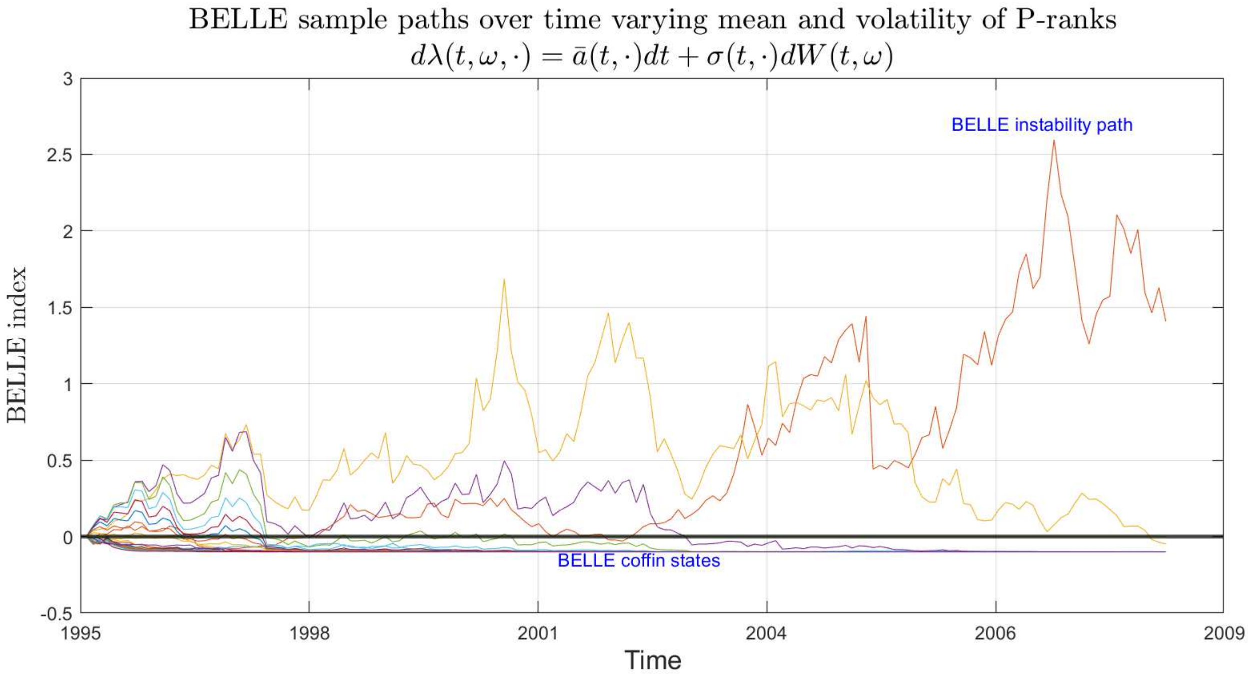

The BELLE process (Theorem 2.1) for 33 sample paths $\lambda(t,\cdot,\omega)$ attain a "coffin state", i.e. attain a constant value $c \in [-0.5, 0]$ at random times $T(\omega)$. The process remains stable in those states where it is "killed" at some random time $T(\omega) \geq \zeta$ when $\lambda(T(\omega),\cdot,) = c$. For example, just before 1998 some sample functions were killed, and just before 2006 another sample function was killed. There are other states that exhibit instability but they are eventually absorbed at the coffin state over time. For example, if the process is stopped at $t = 2006$, then there are two sample paths that exhibit instability because they are above 0 and they are not killed. However, one of those sample paths is absorbed by a coffin state after 2008 while the other path, i.e. $\sup_{\{0<t<\infty\}} \lambda(t,\cdot,\omega)$, is explosive over the entire sample period. That is the path which characterizes market crash.

Probability phase shift in decision makers sentiment

Figure 8: Probability phase shift in decision makers sentiment

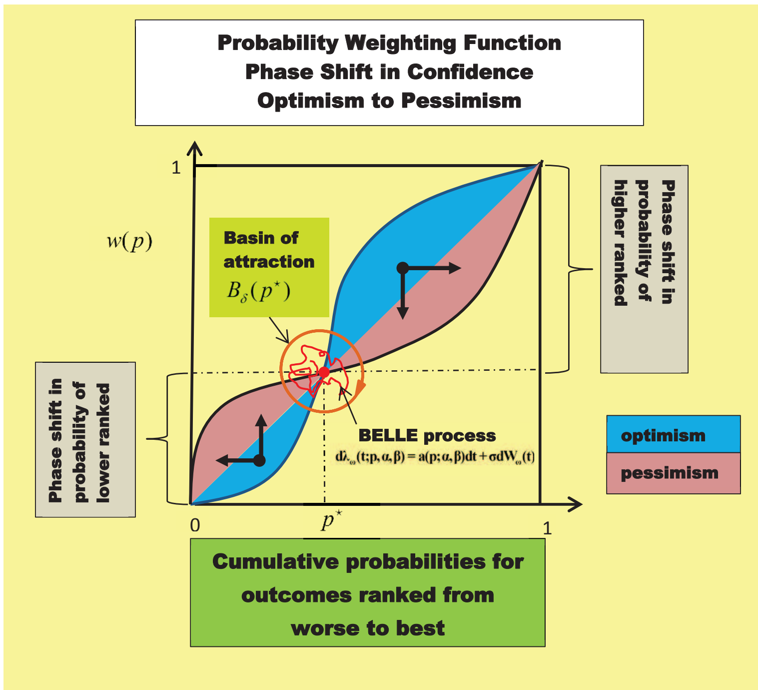

The BELLE process (Theorem 2.1) in the basin of attraction $B_\delta(p^\star)$ characterizes local stochastic stability of the pwfs induced by shifts in DMs sentiment. In the case of a single interior fixed point like that depicted here the BELLE process can be used to obtained closed form expressions for probability of instability arising from large deviations as shown in Theorem 2.2.

Average probability of tail event instability for a seemingly stable behavioural dynamical system

Figure 9: Average probability of tail event instability for a seemingly stable behavioural dynamical system

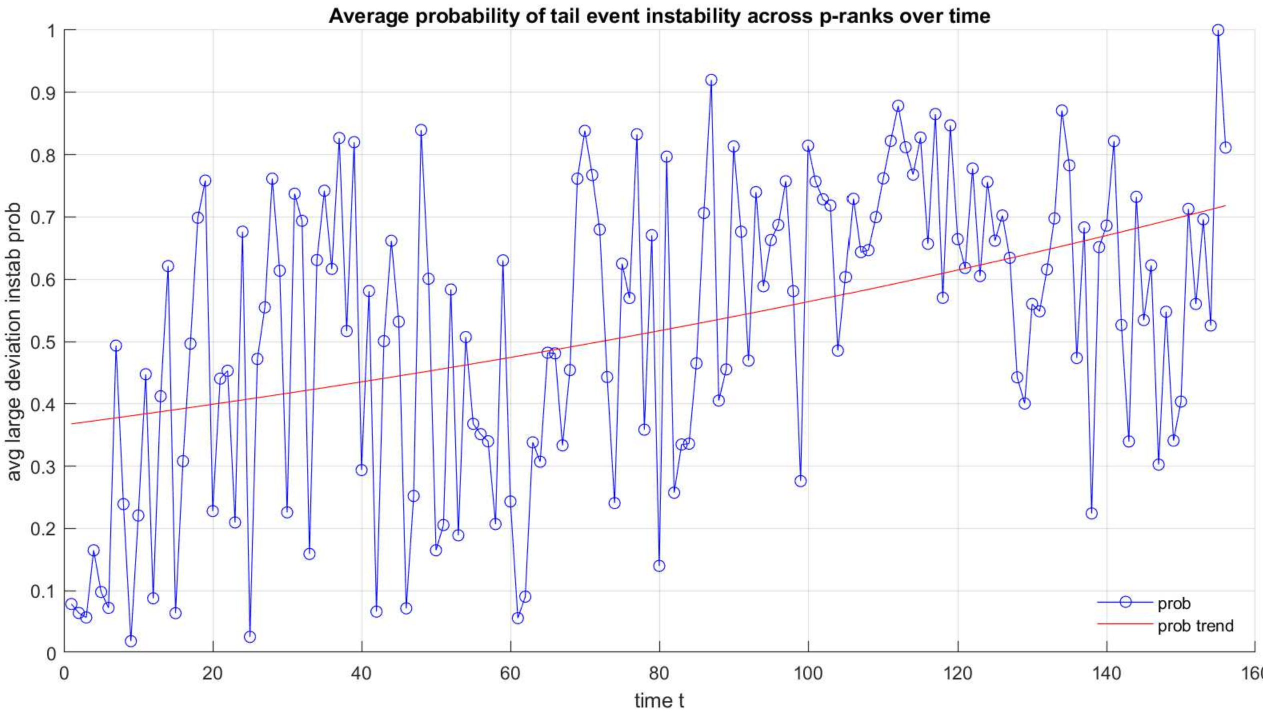

Source: Author's computation from pwf calibrated with data from Polkovnichenko and Zhao (2013, Fig. 6) for CRRA index $\gamma = 0$. Sample function for average stationary transition probability of market instability based on $T = 156$ simulations, under uniform distribution assumption $\sigma \sim \sqrt{2} * \mathcal{U}(0.02, 0.1)$ (cf., Majumdar et al., 2018) for closed form formula in Theorem 2.2. The averages for stationary transition probabilities of instability, across probability ranks, has an upward trend over time as expected. $T = 156$ is the length of the underlying monthly series.

Large deviation probability field

Figure 10: Probability of instability over time across p-rank space

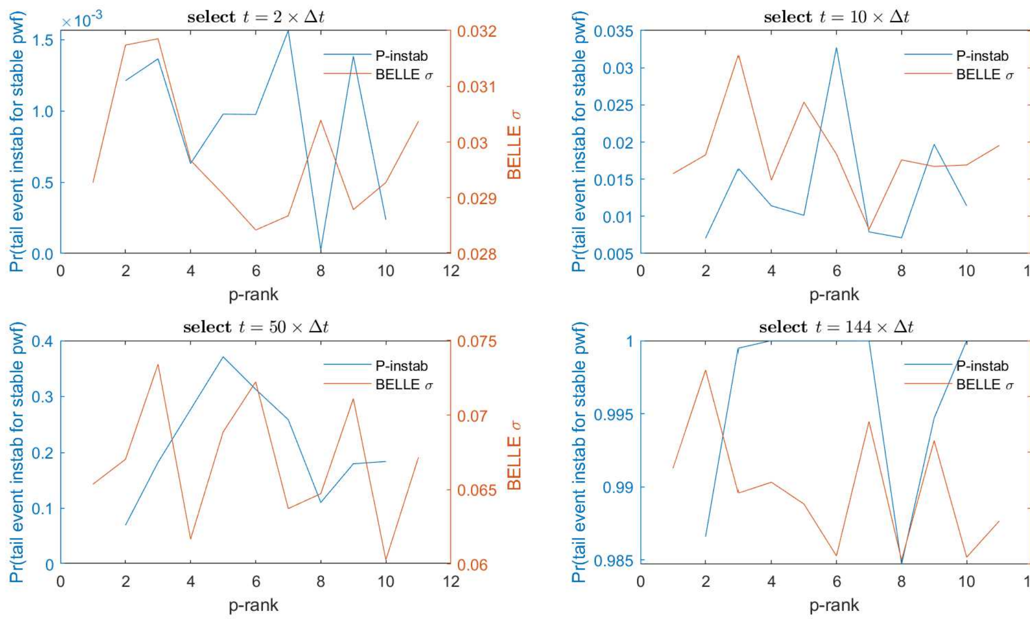

Figure 11: Probability of instability over p-rank space and across time

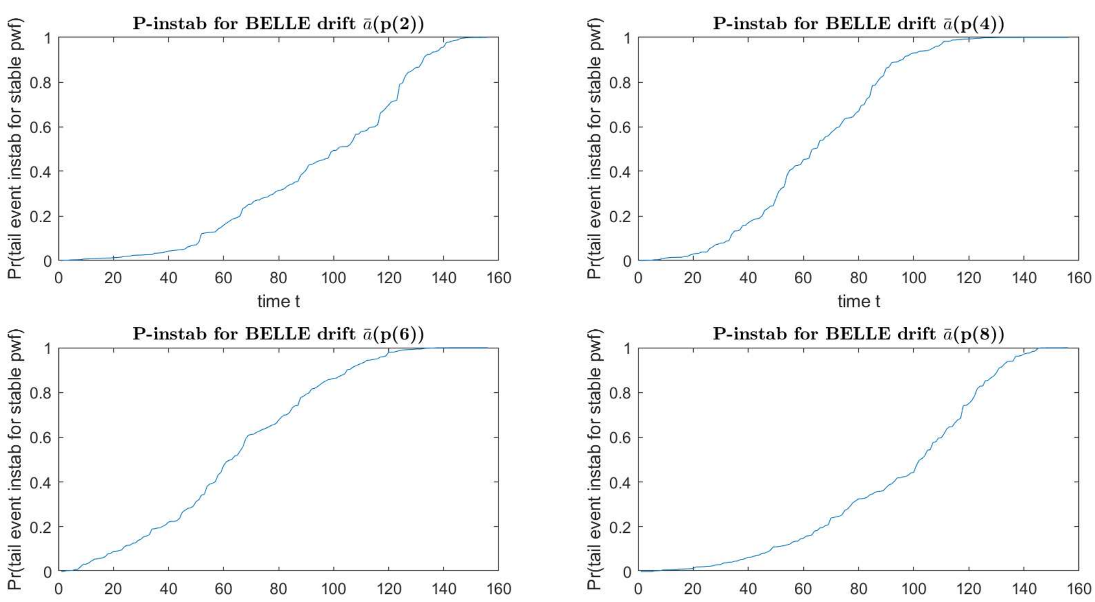

Cross section of simulated random field of stationary transition probability of instability $P_{us}(t, p)$ for tail events, over windowed time t and probability (p) ranks. In Figure 10 for $\Delta t = 1/T \approx 0.006$ for $T = 156$ months of data and $\sigma \sim \sqrt{2} * \mathcal{U}(0.02, 0.1)$ we take snap shots at $2\Delta t, 10\Delta t, 50\Delta t, 144\Delta t$, across probability ranks (p-rank space) over $[0, 1]$ for ranks in increments of 0.1. In Figure 11 we take snapshots of transition probabilities for p-ranks at$k = 2, 4, 6, 8$ for $p \in \{0, 0.1, 0.2, 0.3, 0.4, 0.5, \ldots, 1.0\}$ where $p(1) = 0$ and $p(11) = 1$. The effective ranks for the 10 probabilities are $p(2) \ldots, p(11)$. The range for $P_{us}(t, p)$ is on the vertical axis. As the time window in Figure 10 gets larger, market volatility also increase, and the probability of a crash increases. In Figure 11 the probability of a crash increases over time across all probability ranks.

CBOE VIX Monthly Index: 1/1/1996-12/1/2008

Figure 12: CBOE VIX Monthly Index: 1/1/1996-12/1/2008

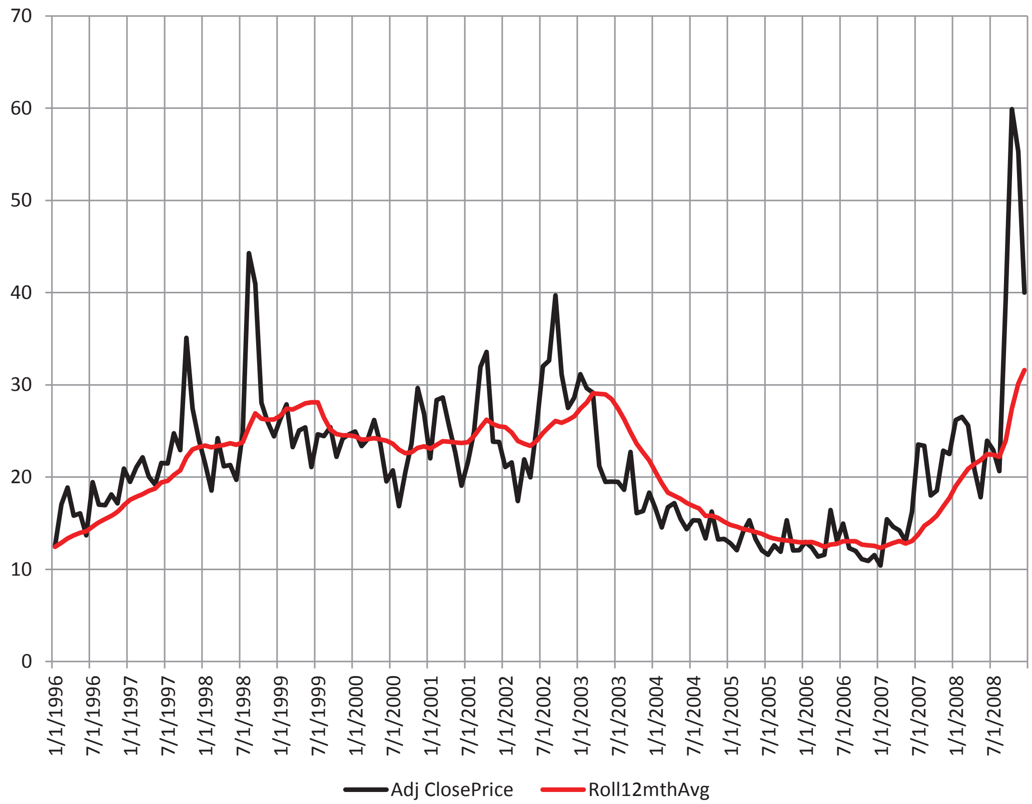

Data source: Yahoo
VIX volatility index as a measure of implied risk aversion in the index option market.

Sample functions over probability ranks for stable and unstable source functions

Figure 13: Sample source functions implied by S&P index option prices

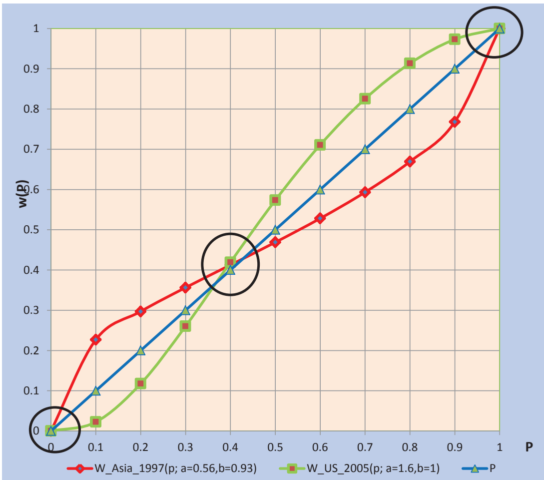

Figure 14: $\beta(p)$-instability $\in$ distribution with tipping points at p=0.4

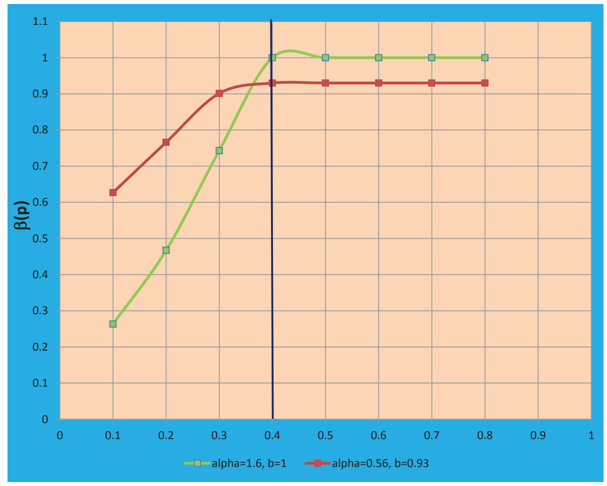

Figure 15: $\beta(p)$ instability $\in$ (0.6, 0.2) for 1997 Asia and 2005 US risk sources

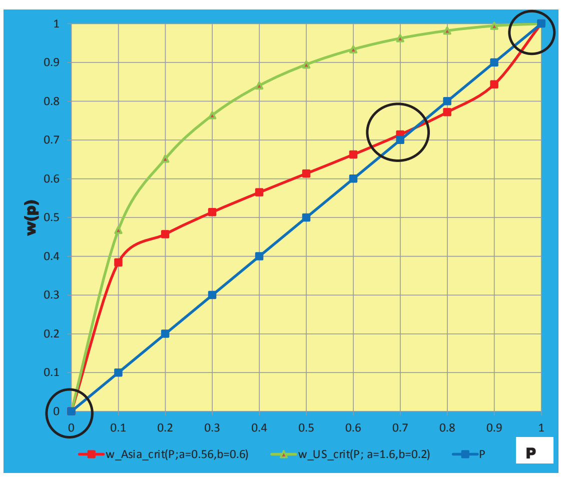

Figure 16: $\beta(p)$-instability $\in$ (0.7, 0.5) for 1997 Asia and 2005 US risk sources

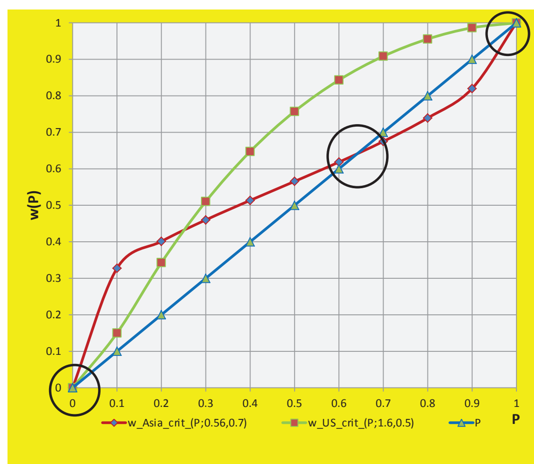

Figure 13 is calibrated with Polkovnichenko and Zhao (2013) estimates for Prelec (1998) 2-parameter source functions for 1997 Asian currency crisis ($\alpha = 0.56, \beta = 0.93$) and 2005 US real estate and CDO bubble ($\alpha = 1.6, \beta = 1$) for CRRA parameter $\gamma = 2$. Figure 14 depicts the distribution of critical values for early warning and tipping point for market crash when p=0.4 for each source function. Figure 15 depicts superimposed market instability source functions for market crash for 2005 US real estate and CDO bubble, and for 1997 Asian currency crisis for for $\beta(p) = 0.6, 0.2$ respectively, and Figure 16 depicts same for $\beta(p) = 0.7, 0.5$ respectively.

Time series plot for α discrimination and β attractiveness of bets in index option market

Figure 17: Time series plot for α discrimination and β attractiveness of bets in S&P index option market

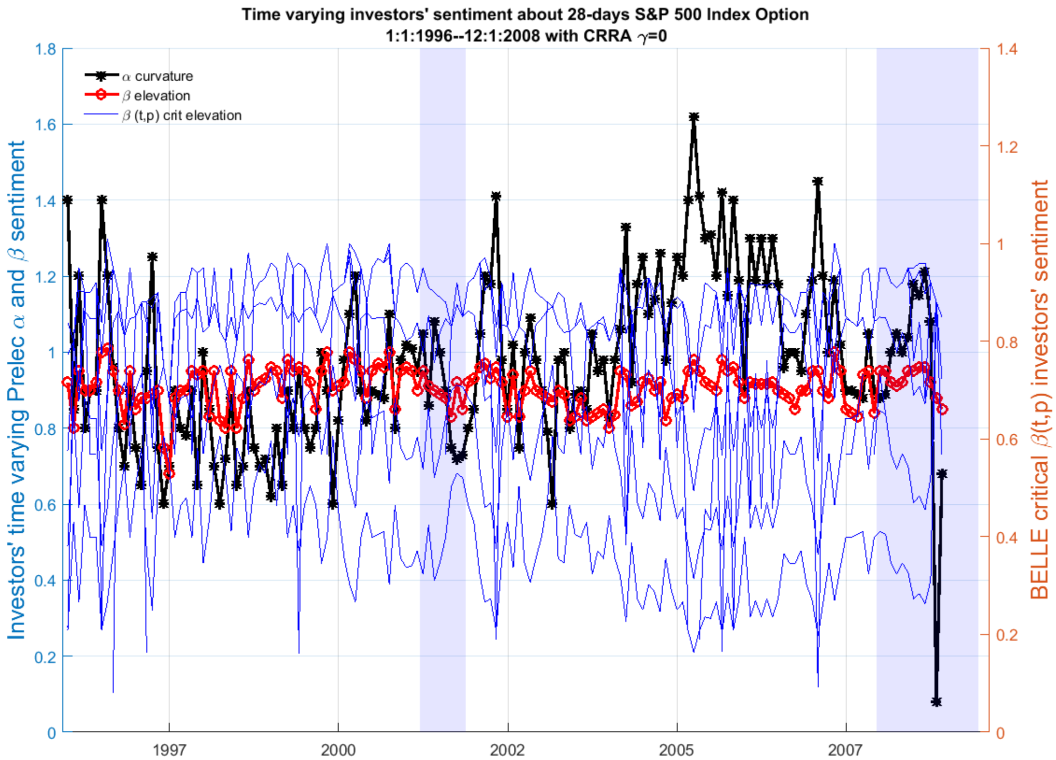

The time series plot is produced from eye balling data in Polkovnichenko and Zhao (2013, Fig. 6, p. 593) for Prelec (1998) α curvature (discrimination), and β elevation (attractiveness) parameters for bets in the S&P index option market when CRRA parameters $\gamma = 0$, i.e. risk neutral utility function. The critical $\beta^{\star}(t, p)$ series (right axis) is computed from the BELLE process. The $\beta^{\star}(t, p)$ series indicates much greater uncertainty and unattractiveness of bets about market crash overtime compared to the α and β series measures on the left axis.

Critical $\beta(p)$ attractiveness of bet sentiment index for market instability and toxic assets with market crash tent maps

Figure 18: Critical $\beta(p)$ sentiment for market instability and toxic assets

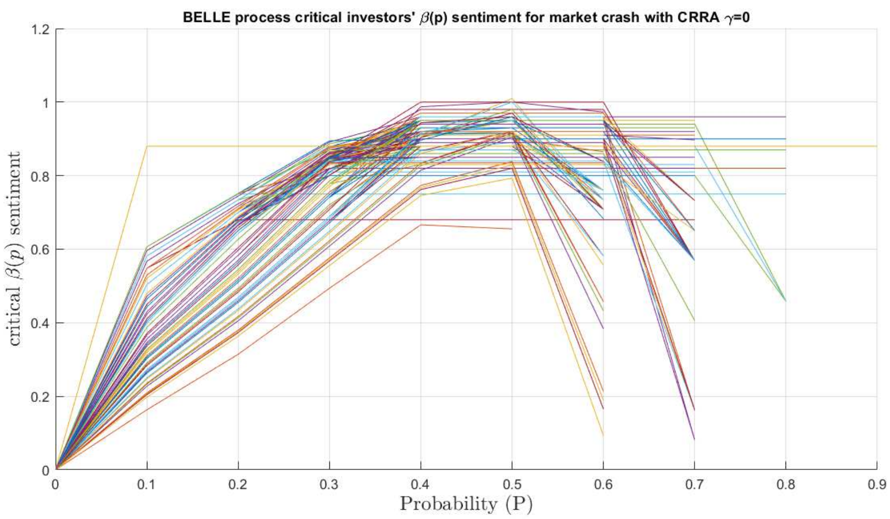

Figure 19: Market crash source functions morph into tent maps

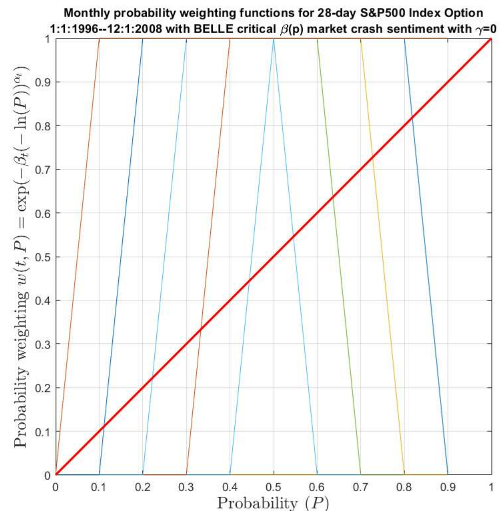

Figure 18 depicts the $\beta(p)$ instability plots for fixed t over the probability distribution for ranked but unattractive index option prices. Figure 19 shows the orientation of the source functions generated by the $\beta(p)$ instability. In every case, the orientation is concave with trapezoid shape and unstable. The limit tent-map, symbolic of chaos, depicts market crash at the critical point $p = 0.5$.

AAII weekly sentiment survey: July 1987–December 2021

Figure 20: AAII weekly sentiment survey: July 1987–April 2021

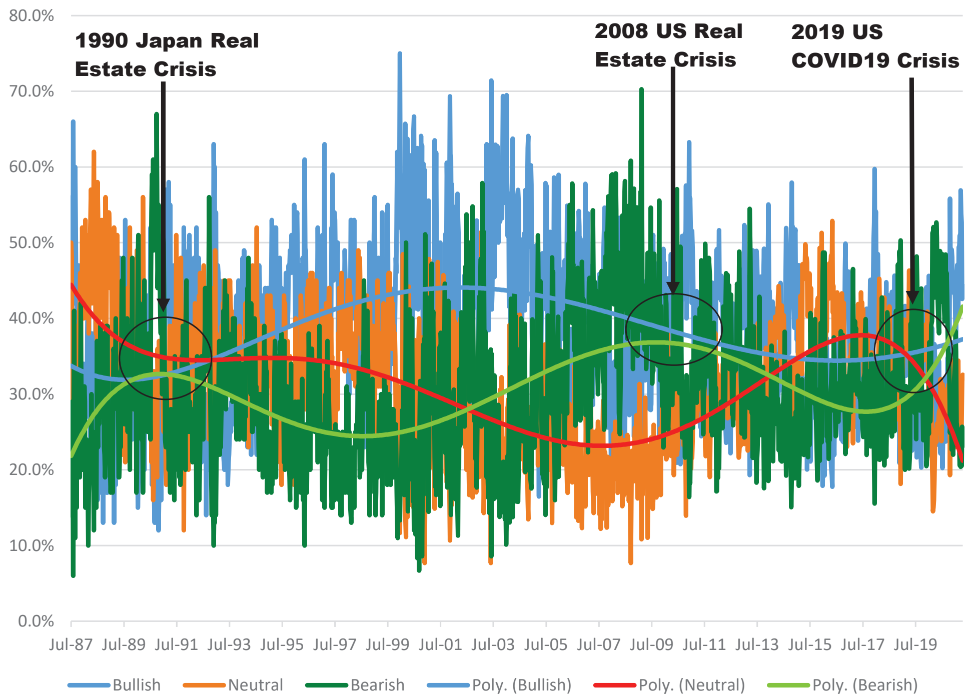

"The AAII Investor Sentiment Survey measures the percentage of individual investors who are bullish, bearish, and neutral on the stock market for the next six months; individuals are polled from the ranks of the AAII membership on a weekly basis. Only one vote per member is accepted in each weekly voting period." Source: AAII Investor Sentiment Survey. A 5th-degree polynomial smoother was used to generate sentiment waves. The Japan Real Estate market crash of 1990 and the COVID-19 induced crash of 2019 are characterized by Bulls, Bears and Neutral sentiment agreement in a circle of agreement. The Great Recession of 2008 is characterized by Bulls and Bears sentiment agreement in a circle of agreement. *Each crisis is characterized by different sentiment dynamics*:

1990 Japan Real Estate Crisis Bear peak meets Bull trough. Market neutral trough higher than both.

2008 US Real Estate Crisis Bear peak meets Bull trough. Market neutral trough lower than both but trending upwards.

2019 US COVID19 Crisis Bears cut Bulls from below and Bulls beginning to rise from low. Market neutral trending downwards below Bears and Bulls.

Market Crash Dynamics–Snapshots of a crash

Figure 21: Market Crash Dynamics–Snapshots of a crash

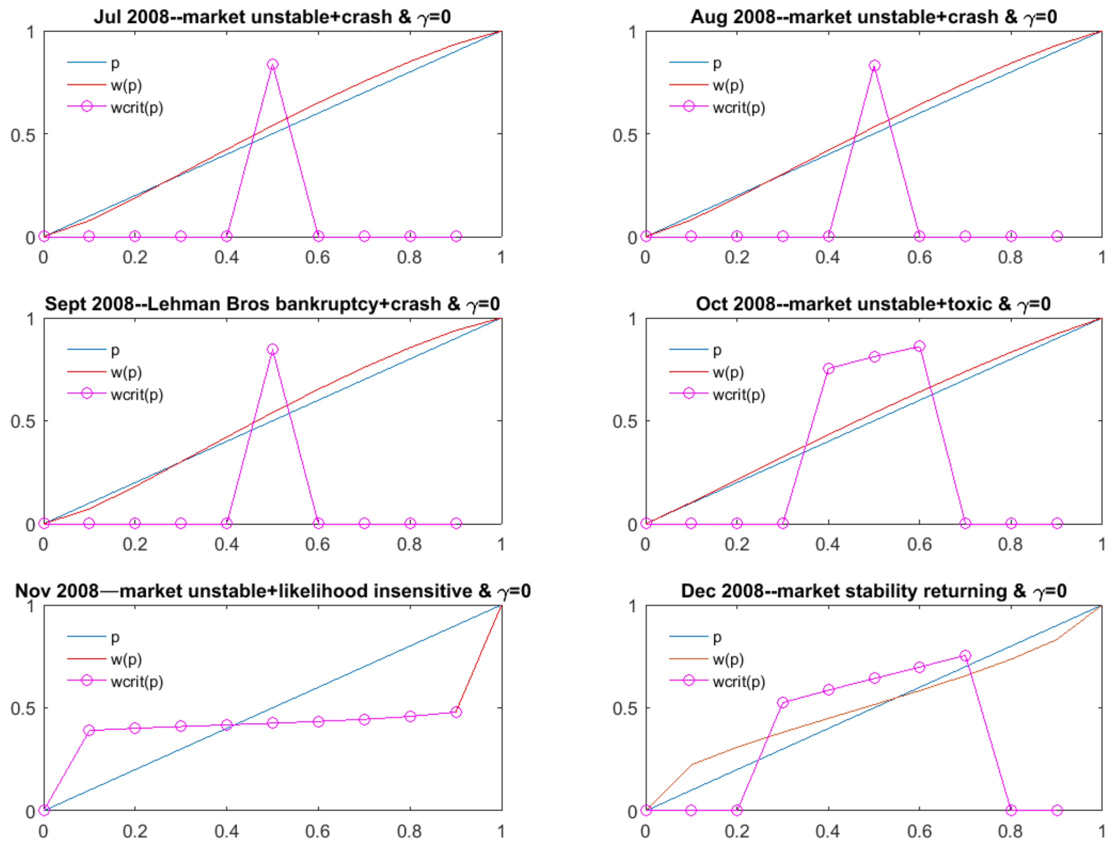

Snap shots of S&P index option market dynamics leading up to and including Lehman Brothers bankruptcy and market crash in 2008. The critical source function plots $wcrit(p)$ with circles signal when the market is about to flip. Tent map signifies chaotic market crash at critical point $p = 0.5$.

G INTERNET APPENDIX

G.1 The stable manifold theorem and preliminaries

This appendix provides some preliminaries and an elementary statement of the stable manifold theorem.

G.1.1 Preliminaries

Definition G.1 (Manifold)**.** "Informally, a manifold is a subset of $\mathbb{R}^n$ such that, for some fixed integer $k \geq 0$, each point in the subset has a neighborhood that is essentially the same as the Euclidean space $\mathbb{R}^k$ ... Points, lines, planes, arcs, spheres, and tori are examples of manifolds." (Chicone, 1999, p. 28). Alternatively, a manifold implies that every point x in an abstract space X can be mapped into a small ball in $\mathbb{R}^m$. The small ball is a m-manifold (McLennan, 2018). Put another way, each point of the m-manifold has a neighbourhood that is homeomorphic to an Euclidean space X.

Definition G.2 (Qualities of a dynamical system)**.** A dynamical system is a system that evolves in time through the iterated application of an underlying dynamical rule. That transition rule describes the change of the actual state in terms of itself and possibly also previous states. The dependence of the state transitions on the states of the system itself means that the dynamics is recursive. In particular, a dynamical system is not a simple input-output transformation, but the actual states depend on the system's own history. In fact, an input need not even be given to the system continuously, but rather it may be entirely sufficient if the input is only given as an initial state and the system is then allowed to evolve according only to its internal dynamical rule. This will represent the typical paradigm of a dynamical system. (Jost, 2005, p. 1). □

Definition G.3 (Dynamical system)**.** (Rebaza, 2012, p. 327).
Let E be an open set in $\mathbb{R}^n$, i.e. $E \subset \mathbb{R}^n$. The function $\phi : \mathbb{R} \times E \to E$ defined by $\phi(t, \mathbf{x}) = \exp(At)\mathbf{x}$ defines a dynamical system on E. Specifically, if $\dot{\mathbf{x}} = A\mathbf{x}$ with initial value $\mathbf{x}(t_0) = \mathbf{x}_0$, then its solution $\mathbf{x}(t) = \exp(At)\mathbf{x}_0$ defines how a state $\mathbf{x} \in E$ evolves over time. If $\mathbf{x} = f(\mathbf{x})$ is a nonlinear system, then $A = \mathbf{D}f(\mathbf{x})$ is the Jacobian for a local linearization. □

Definition G.4 (Invariant subspace)**.** (Rebaza, 2012, p. 338).
A subset $S \subset \mathbb{R}^n$ is called invariant with respect to the system $\dot{\mathbf{x}} = A\mathbf{x}$ if $\exp(At)S \subset S$. For instance, for any initial value $\mathbf{x}(t_0) = \mathbf{x} \in S$, the solution $\mathbf{x}(t) = \exp(At)\mathbf{x}_0$ stays in S for all $t \geq 0$. □

Definition G.5 (Eigenvalue criterion for stability)**.** (Rebaza, 2012, p. 338).
Let $\lambda_j = a_j + ib_j, \;\; j = 1, \ldots, n$ be a complex valued eigenvalue of A in Definition G.3 with eigenvectors $\mathbf{u}_j = \mathbf{v}_j + i\mathbf{w}_j$. Then we define

$$E^s = \operatorname{span}\{\mathbf{v}_j, \mathbf{w}_j : a_j < 0\} \qquad \text{(stable subspace)}$$
$$E^u = \operatorname{span}\{\mathbf{v}_j, \mathbf{w}_j : a_j > 0\} \qquad \text{(unstable subspace)}$$
$$E^c = \operatorname{span}\{\mathbf{v}_j, \mathbf{w}_j : a_j = 0\} \qquad \text{(center subspace)}$$

All three subspaces are invariant with respect to the system. Furthermore, they induce the identity

$$E^s \oplus E^u \oplus E^c = \mathbb{R}^n \tag{G.1}$$

The $\oplus$ symbol means that for any $\mathbf{x} \in \mathbb{R}^n$ we have the decomposition $\mathbf{x} = \mathbf{u} + \mathbf{v} + \mathbf{w}$ with $\mathbf{u} \in E^s$, $\mathbf{v} \in E^u$, $\mathbf{w} \in E^c$. □

Definition G.6 (Homeomorphism)**.** A homeomorphism is a function $h : A \to B$ that is a bijection, is continuous and whose inverse is also continuous. □

Definition G.7 (Differentiable manifold)**.** A differentiable manifold of dimension n as a set that is *locally* homeomorphic to the usual Euclidean space $\mathbb{R}^n$. A differentiable manifold is in fact a topological space that generalizes the intuitive and geometric notion of a curve or a surface. Consider for example the one-dimensional space $\mathbb{R}$. (say, the usual x axis). Then a differentiable manifold homeomorphic to it, is the cubic parabola $y = x^3$: It is a continuous deformation of the x axis. □

G.1.2 Statement of stable manifold theorem

In the case of pwfs in this paper the fixed point probability $p^\star$ is an equilibrium point and the neighbourhood $B_\delta(p^\star)$ is differentiable manifold. Without loss of generality, we consider the equilibrium point to be the origin in the following.

Theorem G.1 (Stable manifold theorem)**.** *(Rebaza, 2012, p. 343).*
Let $E \subset \mathbb{R}^n$ be open containing the origin, let $f \in C^1(E)$, and let ϕ_t be the flow $\dot{\mathbf{x}} = f(\mathbf{x})$. Suppose the origin is a hyperbolic equilibrium point and that $A = Df(\mathbf{0})$ has k eigenvalues with negative real part and the remaining $n-k$ eigenvalues have positive real part. Then,

(a) *There exists a k-dimensional differentiable manifold S tangent to E^s at the origin, such that $\phi_t(S) \subset S, \forall t \geq 0$ and $\lim_{t\to\infty} = 0, \forall x \in S$.*

(b) *There exists a $(n-k)$-dimensional differentiable manifold S tangent to E^u at the origin, such that $\phi_t(U) \subset U, \forall t \leq 0$ and $\lim_{t\to\infty} = 0, \forall x \in U$.*

□

G.2 Positioning the paper in the literature

Active research on financial market instability is conducted under rubric of several genres: market microstructure,[24] econophysics,[25] macrofinance,[26] agent based models,[27] experi-

[24] (Easley et al., 2011; Aldridge, 2014)
[25] Johnson et al. (2000); Zhou and Sornette (2006); Quax et al. (2013)
[26] Abreu and Brunnermeier (2003); Grasselli and Costa Lima (2012); Angeletos and La'O (2013); Keen (2013); Wigniolle (2014)
[27] Thurner et al. (2012); Hommes (2013); Poledna et al. (2014)

mental finance,[28] financial networks,[29] bank runs,[30] debt-deflation cycles,[31] revolving doors,[32] and creative destruction in financial markets.[33] However, none of the papers in those genres use probability weighting functions (pwfs) to characterize financial market instability–even though pwfs reflect sentiments like pessimism and optimism in the presence of risk and uncertainty–common cores of all financial crises (Fisher, 1933; Kindleberger and Aliber, 2011). Bhattacharya et al. (2015) model Minsky's financial instability hypothesis in the context of financial institutions' optimism, leverage, and portfolio risk as part of a debt-deflation cycle.[34] A series of papers by P.C.B Phillips and his co-workers devise econometric tests for market bubbles that take investor mood swings into account. See e.g. Phillips and Yu (2011); Phillips et al. (2011); Phillips (2016); Phillips and Shi (2017). Again, none of the aforementioned authors used pwfs to characterize market sentiment or states of the economy.

*** Insert Figure 22 about here ***

This paper's contribution lies in a novel behavioural empirical local Lyapunov exponent[35] (BELLE) process that characterizes financial market instability with probabilistic risk attitudes implied by index option prices. The latter allow natural experiments on probabilistic risk attitudes because they involve bets on future price movements. Figure 22 depicts the shape of investor sentiment about S&P credit rating for convertible bonds for a sample of firms. The shape resembles a source function for ranked outcomes of lotteries, see e.g. Lopes (1981, 1990), and it also resembles a harmonic tangent function that is periodic in letter ranks. Cf., harmonic source function in Charles-Cadogan (2018). The sinusoidal pattern is employed in Andersson and Vanini (2010) to model credit rating migration in concert with business cycles.

Time dependent *behavioural error* in the orbit of source functions induce a local empirical process[36] for Lyapunov exponents in fixed point probability neighbourhoods as shown *infra*. This facilitates estimation of critical values for investor probabilistic risk attitude factors from closed form expressions for the probability that a stable source function becomes unstable and *vice versa*. We calibrate the model with data from Polkovnichenko and Zhao (2013), and illustrate its robustness in a natural experiment across risk sources for the 1997 Asian currency crisis, 2005 US real estate and CDO bubble, and Great Recession of 2008. We prove that risk source functions implied by index option prices provide early warning of financial market instability, and that they are sufficient statistics for a behavioural version of Minsky's financial instability hypothesis: An economy has stable and unstable regimes, and it transits from financial relations that make it stable to those that make it unstable (Minsky (1986, pp. 173-174) and Minsky (1994)).

[28] Smith et al. (1988); Ackert et al. (2009); Ashparouva et al. (2016)

[29] Allen and Gale (2000); Acemoglu et al. (2015)

[30] Diamond and Dybvig (1983)

[31] Fisher (1933); Bhattacharya et al. (2015)

[32] Charles-Cadogan and Cole (2014); Shive and Forster (2017); Lucca et al. (2014); Lambert (2017)

[33] Minsky (1986)

[34] Shefrin (2016) provides a qualitative model that deals with similar issues.

[35] A Lyapunov exponent (λ) is a measure of the rate of convergence or divergence of a trajectory over time relative to two nearby starting points

[36] A classic empirical process is one comprised of sums of independent and identically distributed (*iid*) random variables (in our case noise) that converge to a limit process (Shorack and Wellner, 1986, pp. 1, 24).

*** Insert Figure 23 and Figure 24 about here ***

Figure 23 and Figure 24 depict the topology of our model. For example, the phase portrait in Figure 23 depicts the concave-convex shape of a stable source function associate with probabilistic risk aversion.[37] Whereas Figure 24 depicts the convex-concave shape of an unstable source function associated with probabilistic risk seeking or "irrational exuberance". Each curve is characterized by curvature (α) and elevation (β) parameters that reflect DMs sentiment in Prelec's (1998) 2-parameter source function $w(p) = \exp(-\beta(-\ln(p))^{\alpha})$. According to Gonzalez and Wu (1999), α is a measure of discrimination among bets, while β measures the attractiveness of a bet. This psychological probabilistic measure of attractiveness is distinguished from the utility based approach in Dierkes et al. (2010).

Figure 1 depicts a field of stable and unstable source functions over time in the S&P 500 index option market, i.e. $w(t,p) = \exp(-\beta_t(-\ln(p))^{\alpha_t})$ for $t \in \{t_1, \ldots, t_n\}$ in an index set for data over time (in months), and $p \in \{p_1, \ldots, p_m\}$ in a set of probability ranks. Behavioural dynamics in fixed point probability neighourhoods $B_\delta(p^\star)$ centered at fixed-point $p^\star$ with radius δ, control the shape of source functions, and determine phase transition of stable and unstable source functions shapes.[38] We endow $B_\delta(p^\star)$ with a canonical probability measure space $(\Omega, \mathscr{F}, P)$, and construct a behavioural local Lyapunov exponent (BELLE) process $\{\lambda(t,p,\omega); t \geq 0\}$ in $B_\delta(p^\star)$, accordingly. The latter is a random field that characterizes stochastic stability of source functions over time and probability ranks, and we calibrate it to risk source functions implied by index option prices over time as shown in Figure 1. The outlier function depicts likelihood insensitivity in November 2008. See Figure 21, *infra*. The sign of $\{\lambda(t,p,\omega); t \geq 0\}$ determines stability (negative sign) or instability (positive sign) of the underlying source function.

[37] The stability of risk aversion is rooted in evolutionary biology (See e.g. Zhang et al., 2014; Hintze et al., 2015).

[38] $B_\delta(p^\star)$ is also called the domain or basin of attraction of $p^\star$. Refer to Medio and Lines (2003, Ch. 3) for details on stable and unstable fixed points.

G.3 Figures

Ratio of Stock Price to Exercise Price (S/X) sorted by S&P Ratings

Figure 22: Ratio of Stock Price to Exercise Price (S/X) sorted by S&P Ratings

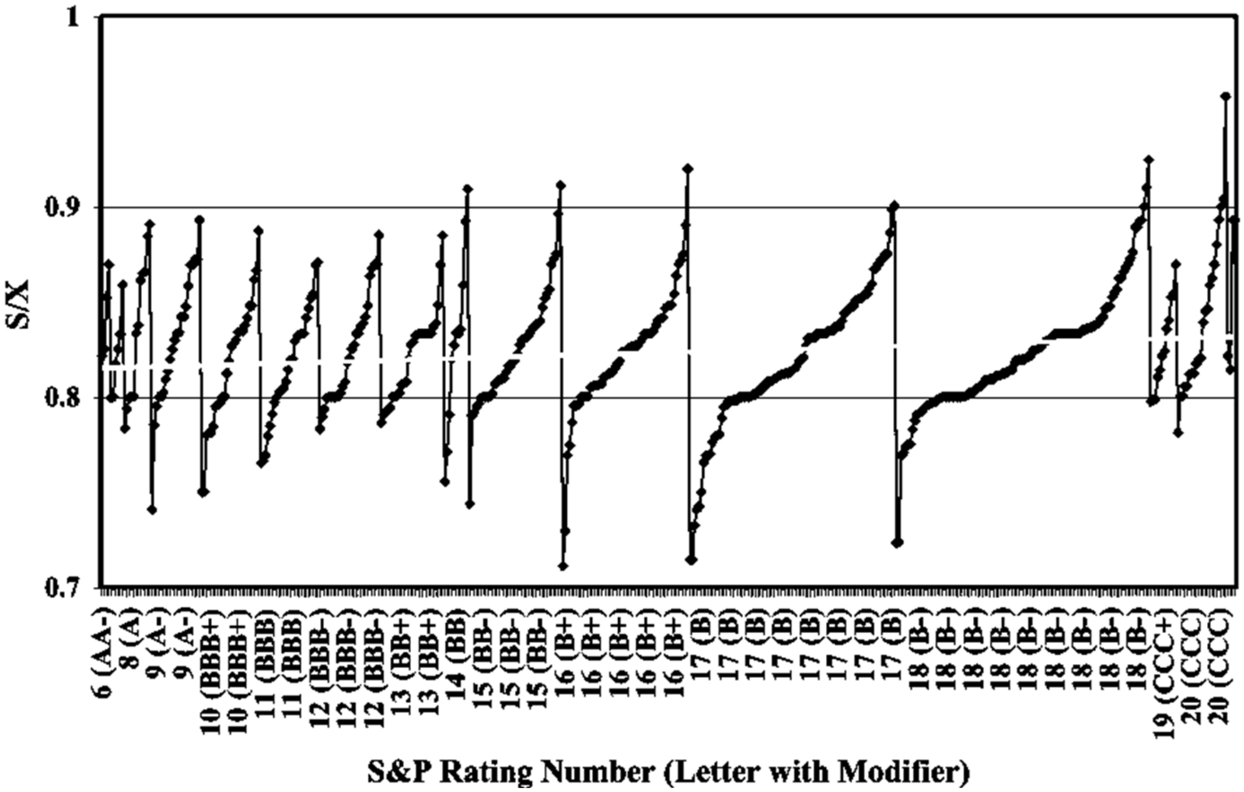

Source: Ogden et al. (2003). The plot depicts the ratio of stock price to exercise price (S/X) for convertible bonds sorted by S&P Ratings and S/X within ratings for a sample of US nonfinancial firms in 1996. The shapes reflect decision makers' (DMs) probabilistic risk attitudes about the ranked ratings. Even within the same S&P ratings DMs tend to distort probabilities.

Stable and unstable pwfs

Figure 23: Stable pwf

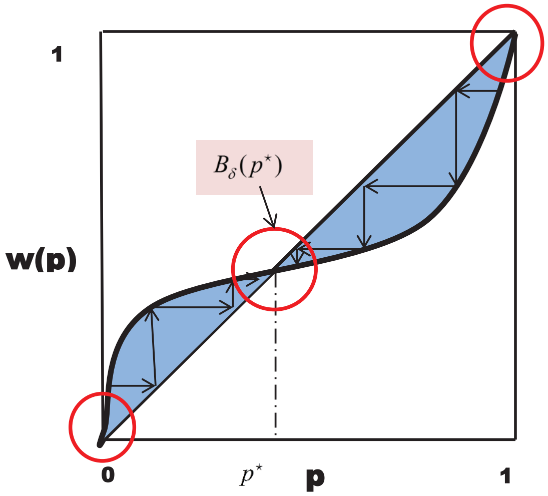

Figure 24: Unstable pwf

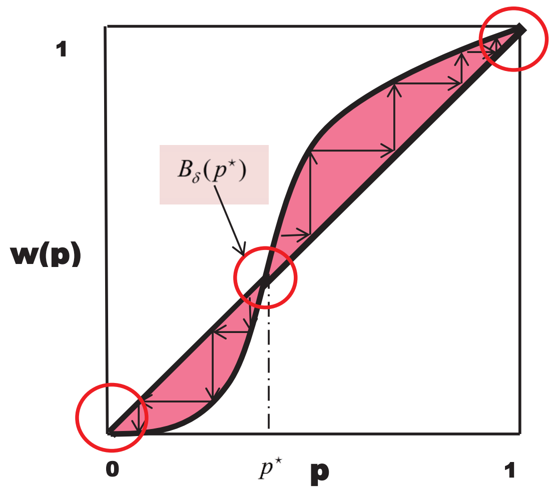

Phase diagrams for stable and unstable pwfs $w(p)$. The BELLE process $\{\lambda(t, p, \omega); t \geq 0\}$ in fixed point $(p^\star)$ probability neighbourhood $B_\delta(p^\star)$ characterizes the dynamics of pwfs. If $\lambda(t, p, \omega) < 0$ in $B_\delta(p^\star)$ the process is stable and unstable otherwise. The stable pwf is in-phase, i.e. the isoclines are moving in the same direction towards the stable fixed point. While the unstable pwf is anti-phase, i.e. isoclines are moving away from the fixed point.

References

Abdellaoui, M., A. Baillon, L. Placido, and P. Wakker (2011, Apr). The Rich Domain of Uncertainty: Source Functions and their Experimental Implementation. *American Economic Review 101*(2), 695–723.

Abreu, D. and M. K. Brunnermeier (2003). Bubbles and crashes. *Econometrica 71*(1), 173–204. http://doi.org/10.1111/1468-0262.00393.

Acemoglu, D., A. Ozdaglar, and A. Tahbaz-Salehi (2015). Systemic risk and stability in financial networks. *American Economic Review 105*(2), 564–608.

Ackert, L. F., N. Charupat, R. Deaves, and B. D. Kluger (2009). Probability judgment error and speculation in laboratory asset market bubbles. *Journal of Financial and Quantitative Analysis 44*(3), 719–744. https://doi.org/10.1017/S0022109009990019.

Adelson, M. (2013, Spring). The Deeper Causes of The Financial Crisis: Mortgages Alone Cannot Explain It. *Journal of Portfolio Management*, 1–16.

Akbas, F. and E. Genc (2020). Do mutual fund investors overweight the probability of extreme payoffs in the return distribution? *Journal of Financial and Quantitative Analysis 55*(1), 223–261. https//doi.org/10.1017/S0022109018001345.

Akerlof, G. A. (1970, Aug). The market for 'lemons': quality uncertainty and the market mechanism. *Quarterly Journal of Economics 84*(3), 488–500.

Aldridge, I. (2014). High-Frequency Runs and Flash-Crash Predictability. *Journal of Portfolio Management 40*(3), 113–123.

Allen, F. and D. Gale (2000, Feb). Financial Contagion. *Journal of Political Economy 108*(1), 1–33.

Altman, E. I. (1998). The importance and subtlety of credit rating migration. *Journal of Banking & Finance 22*(10), 1231 – 1247. https://doi.org/10.1016/S0378-4266(98)00066-1.

Andersson, A. and P. Vanini (2010, Mar). Credit migration risk modelling. *Journal of Credit Risk 6*(1). https://doi.org/10.21314/JCR.2010.104.

Angeletos, G.-M. and J. La'O (2013). Sentiments. *Econometrica 81*(2), 739–779. http://dx.doi.org/10.3982/ECTA10008.

Arnold, V. I. (1984). *Ordinary Differential Equations* (3rd ed.). Universitext. New York, NY: Springer-Verlag.

Ashparouva, E., P. Bossaerts, and A. Tran (2016, Jan). Market Bubbles and Crashes as an Expression of Tension Between Social and Individual Rationality. Working Paper, Dep't of Finance, Eccles School of Business, Univ. of Utah. Available at http://uleef.business.utah.edu/newsite/RPT1/C_Papers/paper13_working_decision3.pdf. Last visited 6/23/2020.

Baele, L., J. Driessen, S. Ebert, J. M. Londono, and O. G. Spalt (2019, Sep). Cumulative Prospect Theory, Option Returns, and the Variance Premium. *Review of Financial Studies 32*(9), 3667–3723. https://doi.org/10.1093/rfs/hhy127.

Barberis, N. C. (2013, September). Thirty Years of Prospect Theory in Economics: A Review and Assessment. *Journal of Economic Perspectives 27*(1), 173–96. http://doi.org/10.1257/jep.27.1.173.

Baucells, M. and F. H. Heukamp (2012). Probability and time trade–off. *Management Science 58*(4), 831–842.

Ben Saïda, A. (2012). Are financial markets stochastic: A test for noisy chaos. *Am Int J Contemp Res 2*(8), 57–68.

Ben Saïda, A. (2014). Noisy chaos in intraday financial data: Evidence from the American index. *Applied Mathematics and Computation 226*(0), 258 – 265.

Bhattacharya, S., C. A. E. Goodhart, D. P. Tsomocos, and A. P. Vardoulakis (2015, Aug). A Reconsideration of Minsky's Financial Instability Hypothesis. *Journal of Money Credit and Banking 47*(5), 931–973.

Black, F. and M. Scholes (1973, May-Jun). The Pricing of Options and Corporate Liabilities. *Journal of Political Economy 81*(3), 637–654.

Bougerol, P. and N. Picard (1992). Stationarity of GARCH processes and of some nonnegative time series. *Journal of Econometrics 52*(1–2), 115 – 127.

Brock, W. A. and C. H. Hommes (1998). Heterogeneous beliefs and routes to chaos in a simple asset pricing model. *Journal of Economic Dynamics and Control 22*(8–9), 1235 – 1274.

Budescu, D., A. Abbas, and L. Wu (2011). Does probability weighting matter in probability elicitation? *Journal of Mathematical Psychology 55*(4), 320–327.

Campbell, J. Y., A. W. Lo, and A. C. MacKinlay (1997). *The Econometrics of Financial Markets*. Princeton, NJ: Princeton University Press.

Carlé, T. A., Y. Lahav, T. Neugebauer, and C. N. Noussair (2019). Heterogeneity of beliefs and trade in experimental asset markets. *Journal of Financial and Quantitative Analysis 54*(1), 215–245. http://doi/org/10.1017/S0022109018000571.

Cesa-Bianchi, A., F. E. Martin, and G. Thwaites (2018). Foreign booms, domestic busts: The global dimension of banking crises. *Journal of Financial Intermediation*. In press. https://doi.org/10.1016/j.jfi.2018.07.001.

Chabi-Yo, F. and Z. Song (2013, June). Recovering The Probability Weights of Tail Events With Volatility Risk From Option Prices. Working Paper, Department of Finance, Fisher School of Business, Ohio State U.

Charles-Cadogan, G. (2018). Probability interference in expected utility theory. *Journal of Mathematical Economics 78*, 163–175. https://doi.org/10.1016/j.jmateco.2018.03.006.

Charles-Cadogan, G. and J. A. Cole (2014). Bankruptcy Risk Induced By Career Concerns of Regulators. *Financial Research Letters 11*, 259–271.

Chen, H., S. Joslin, and N.-K. Tran (2012, 06). Rare Disasters and Risk Sharing with Heterogeneous Beliefs. *Review of Financial Studies 25*(7), 2189–2224. https://doi.org/10.1093/rfs/hhs064.

Chen, Y. and S. Xuefeng (2003). Study on the chaos model of liquidity in the stock market. *Systems Research and Behavioral Science 20*(5), 419–425.

Chicone, C. C. (1999). *Ordinary Differential Equations With Applications*, Volume 34 of *Texts in Applied Mathematics*. New York, NY: Springer.

Chung, K. L. (1960). *Markov chains with stationary transition probabilities*, Volume 104 of *Grundlehren der Mathematischen Wissenschaften*. Berlin: Springer-Verlag.

Corsetti, G., P. Pesenti, and N. Roubini (1999). What caused the Asian currency and financial crisis? *Japan and the World Economy 11*(3), 305–373.

De Long, J. B., A. Shleifer, L. H. Summers, and R. J. Waldmann (1990). Noise trader risk in financial markets. *Journal of political Economy 98*(4), 703–738. https://doi.org/10.1086/261703.

Diamond, D. W. and P. H. Dybvig (1983, Jan). Bank runs, deposit insurance, and liquidity. *Journal of Political Economy 91*(3), 401–419. https://doi.org/10.1086/261155.

Dierkes, M. (2009, Nov). Option Implied Risk Attitude Under Rank Dependent Utility. Working Paper, Finance Center, Univ. Münster, Germany.

Dierkes, M. (2013, Apr). Probability Weighting And Asset Prices. Working Paper, Finance Center, Univ. Münster, Germany.

Dierkes, M., C. Erner, and S. Zeisberger (2010). Investment horizon and the attractiveness of investment strategies: A behavioral approach. *Journal of Banking & Finance 34*(5), 1032 – 1046. https://doi.org/10.1016/j.jbankfin.2009.11.003.

Dierkes, M., S. Germer, and V. Sejdiu (2020). Probability distortion, asset prices, and economic growth. *Journal of Behavioral and Experimental Economics 84*, 101476. https://doi.org/10.1016/j.socec.2019.101476.

Drago, D. and R. Gallo (2017). The impact of sovereign rating changes on European syndicated loan spreads: The role of the rating-based regulation. *Journal of International Money and Finance 73*, 213 – 231. https://doi.org/10.1016/j.jimonfin.2017.02.029.

Dynkin, E. B. (1960). *Theory of Markov Process*. Oxford,UK: Pergamon Press. Translated from Russian.

Easley, D., M. M. López De Prado, and M. O'Hara (2011). The Microstructure of the "Flash Crash": Flow Toxicity, Liquidity Crashes, and the Probability of Informed Tradding. *Journal of Portfolio Management 37*(2), 118–128.

Financial Crisis Inquiry Comission (2011, Jan). The Financial Crisis Inquiry Report: Final Report Of The National Commission On The Causes Of The Financial And Economic Crisis In The United States. Technical report, National Commission on the Causes of the Financial and Economic Crisis in the United States, Washington, DC. Superintendent of Documents, U.S. Government Printing Office.

Finnerty, J. D., C. D. Miller, and R. Chen (2013). The impact of credit rating announcements on credit default swap spreads. *Journal of Banking & Finance 37*(6), 2011 – 2030. https://doi.org/10.1016/j.jbankfin.2013.01.028.

Fisher, I. (1933, Oct). The Debt-Deflation Theory of Great Depression. *Econometrica 1*(4), 337–357.

Fox, C. R., B. A. Rogers, and A. Tversky (1996). Options traders exhibit subadditive decision weights. *Journal of Risk and Uncertainty 13*(1), 5–17.

Furstenberg, H. and H. Kesten (1960). Products of random matrices. *Annals of Mathematical Statistics 31*(2), 457–469. https://www.jstor.org/stable/2237962.

Giglio, S., M. Maggiori, J. Stroebel, and S. Utkus (2021, May). Five Facts about Beliefs and Portfolios. *American Economic Review 111*(5), 1481–1522. http://doi.org/10.1257/aer.20200243.

Gihman, I. I. and A. V. Skorohod (1972). *Stochastic Differential Equations*. Number 72 in Mathematics and Its Applications. New York, NY: Springer-Verlag.

Gikhman, I. I. and A. V. Skorokhod (1969). *Introduction to The Theory of Random Processes*. Phildelphia, PA: W. B. Saunders, Co. Dover reprint 1996.

Gonzalez, R. and G. Wu (1999). On the shape of the probability weighting function. *Cognitive Psychology 38*(1), 129–166. https://doi.org/10.1006/cogp.1998.0710.

Grasselli, M. and B. Costa Lima (2012). An analysis of the Keen model for credit expansion, asset price bubbles and financial fragility. *Mathematics and Financial Economics 6*(3), 191–210.

Haigh, M. S. and J. A. List (2005). Do professional traders exhibit myopic loss aversion? an experimental analysis. *Journal of Finance 60*(1), 523–534.

Harris, M. and A. Raviv (1993). Differences of Opinion Make a Horse Race. *Review of Financial Studies 6*(3), 473–506.

He, X. and X. Zhou (2016). Hope, Fear, And Aspirations. *Mathematical Finance 26*(1), 3–50. http://dx.doi.org/10.1111/mafi.12044.

Heston, S. L. (1993). A closed-form solution for options with stochastic volatility with applications to bond and currency options. *Review Of Financial Studies 6*(2), 327–343. https://doi.org/10.1093/rfs/6.2.327.

Hey, J. D. (1995). Experimental investigations of errors in decision making under risk. *European Economic Review 39*(3–4), 633 – 640. Papers and Proceedings of the Ninth Annual Congress European Economic Association.

Hintze, A., R. S. Olson, C. Adami, and R. Hertwig (2015). Risk sensitivity as an evolutionary adaptation. *Scientific Reports 5*(8242), 1–7. http://dx.doi.org/10.1038/srep08242.

Hogarth, R. M. and H. J. Einhorn (1990, Jul). Venture Theory: A Model of Decision Weights. *Management Science 36*(7), 780–803.

Hommes, C. (2013). *Behavioral Rationality and Heterogeneous Expectations in Complex Economic Systems*. New York, NY: Cambridge University Press.

Hommes, C. H. and S. Manzan (2006). Comments on "Testing for nonlinear structure and chaos in economic time series". *Journal of Macroeconomics 28*(1), 169 – 174. Special Issue: Nonlinear Macroeconomic Dynamics.

Hsieh, D. A. (1991). Chaos and Nonlinear Dynamics: Application to Financial Markets. *Journal of Finance 46*(5), 1839–1877. 10.1111/j.1540-6261.1991.tb04646.x.

Ismailescu, I. and H. Kazemi (2010). The reaction of emerging market credit default swap spreads to sovereign credit rating changes. *Journal of Banking & Finance 34*(12), 2861 – 2873. https://doi.org/10.1016/j.jbankfin.2010.05.014.

Jackwerth, J. (2020, Aug). What Do Index Options Teach Us About COVID-19? *Review of Asset Pricing Studies 10*(4), 618–634. https://doi.org/10.1093/rapstu/raaa012.

Johnson, A., O. Ledoit, and D. Sornette (2000). Crashes as Critical Points. *International Journal of Theoretical and Applied Finance 3*(2), 219–255.

Jost, J. (2005). *Dynamical Systems: Examples of Complex Behavior*. Universitext. New York, NY: Springer.

Karatzas, I. and S. E. Shreve (1991). *Brownian Motion and Stochastic Calculus*. Graduate Texts in Mathematics. New York, N.Y.: Springer-Verlag.

Keen, S. (2013, Feb.). A monetary Minsky model of the Great Moderation and the Great Recession. *Journal of Economic Behavior & Organization 86*, 221–235.

Kilka, M. and M. Weber (2001, Dec). What determines The Shape of The Probability eighting Function Under Uncertainty? *Management Science 47*(12), 1712–1726.

Kindleberger, C. P. and R. Z. Aliber (2011). *Manias, panics and crashes: A history of financial crises*. New York, NY: Palgrave Macmillan.

Kliger, D. and O. Levy (2010). Overconfident investors and probability misjudgments. *Journal of Socio-Economics 39*(1), 24–29. https://doi.org/10.1016/j.socec.2009.08.007.

Kluger, B. D. and S. B. Wyatt (2004). Are Judgment Errors Reflected in Market Prices and Allocations? Experimental Evidence Based on the Monty Hall Problem. *Journal of Finance 59*(3), 969–997. http://doi.org/10.1111/j.1540-6261.2004.00654.x.

Knight, F. B. (1962, May). On the Random Walk and Brownian Motion. *Transactions of the American Mathematical Society 103*(2), 218–228.

Kuhnen, C. M. (2015). Asymmetric Learning from Financial Information. *Journal of Finance 70*(5), 2029–2062. http://doi.org/10.1111/jofi.12223.

Lambert, T. (2017). Lobbying on Regulatory Enforcement Actions: Evidence from Banking. *Management Science*. Forthcoming.

Leonov, G. A. and N. V. Kuznetsov (2007). Time-Varying Linearization And The Perron Effects. *International Journal of Bifurcation and Chaos 17*(04), 1079–1107.

Loewenstein, G. F., E. U. Weber, C. K. Hsee, and N. Welch (2001). Risk as feelings. *Psychological Bulletin 127*(2), 267.

Lopes, L. L. (1981). Decision making in the short run. *Journal of Experimental Psychology: Human Learning and Memory 7*(5), 377.

Lopes, L. L. (1987). Between Hope and Fear: The Psychology of Risk. *Advances in Experimental Social Psychology 20*(3), 255–295.

Lopes, L. L. (1990). Re-Modeling Risk Aversion: A Comparison Of Bernoullian and Rank Dependent Value Approaches. In G. M. von Furstenberg (Ed.), *Acting Under Uncertainty: Multidisciplinary Conceptions*, Theory and Decision Library. Series A., Philosophy and Methodology of The Social Science, Chapter 11, pp. 267–299. Dordrecht, Netherlands: Kluwer Academic Publishers.

Lopes, L. L. (1995). Algebra and Process in The Modeling of Risky Choice. In J. Busemeyer, R. Hastie, and D. L. Medin (Eds.), *Decision Making From A Cognitive Perspective*, Volume Advances in Research and Theory of *The Psychology of Learning and Motivation*, pp. 177–220. San Diego, CA: Academic Press, Inc.

Lucca, D., A. Seru, and F. Trebbi (2014). The Revolving Door and Worker Flows in Bank regulation. *Journal of Monetray Economics 65*, 17–32.

Majumdar, R., P. Mariano, H. Panzo, L. Peng, and A. Sisti (2018). Lyapunov exponent and variance in the CLT for products of random matrices related to random Fibonacci sequences. Available at https://arxiv.org/abs/1809.02294v1.

McCaffrey, D. F., S. Ellner, A. R. Gallant, and D. W. Nychka (1992, Sep). Estimating the Lyapunov Exponent of a Chaotic System With Nonparametric Regression. *Journal of the American Statistical Association 87*(419), 682–695.

McLennan, A. (2018). *Advanced Fixed Point Theory For Economics*, Volume 25. Springer.

Medio, A. and M. Lines (2003). *Nonlinear Dynamics: A Primer*. New York, NY: Cambridge University Press.

Minsky, H. (1986). *Stabilizing an Unstable Economy*. New Haven, CT: Yale Univ. Press.

Minsky, H. (1994). The financial instability hypothesis. In M. Arestis and M. C. Sawyer (Eds.), *The Elgar Companion To Radical Political Economy*, pp. 153–157. Brookfield, VT: Elgar. Available at Jerome Levy Economics Institute, Bard College. Working Paper No. 74. Available at http://papers.ssrn.com/sol3/papers.cfm?abstract_id=161024.

Mishkin, F. S. (1999). Global Financial Instability: Framework, Events, Issues. *Journal of Economic Perspectives 13*(4), 3–20.

Nychka, D., S. Ellner, A. R. Gallant, and D. McCaffrey (1992). Finding Chaos in Noisy Systems. *Journal of the Royal Statistical Society. Series B (Methodological) 54*(2), 399–426.

Ogden, J. P., F. C. Jen, and P. F. O'Connor (2003). *Advanced Corporate Finance: Policies And Strategies*. New York, NY: Pearson College Division.

Olivieri, E. and M. E. Vares (2005). *Large deviations and metastability*, Volume 100. Cambridge University Press.

Park, J. Y. and Y. Whang (2012). Random walk or chaos: A formal test on the Lyapunov exponent. *Journal of Econometrics 169*(1), 61 – 74. Recent Advances in Panel Data, Nonlinear and Nonparametric Models: A Festschrift in Honor of Peter C.B. Phillips.

Peek, J. and E. S. Rosengren (2000). Collateral Damage: Effects of the Japanese Bank Crisis on Real Activity in the United States. *American Economic Review 90*(1), 30–45.

Phillips, P. C. (2016). Modeling speculative bubbles with diverse investor expectations. *Research in Economics 70*(3), 375 – 387. https://doi.org/10.1016/j.rie.2016.01.002.

Phillips, P. C. and S.-P. Shi (2017). Financial bubble implosion and reverse regression. *Econometric Theory*, 1–49. https://doi.org/10.1017/S0266466617000202.

Phillips, P. C. B., Y. Wu, and J. Yu (2011). Explosive Behavior In The 1990S NASDAQ: When Did Exuberance Escalate Asset Values? *International Economic Review 52*(1), 201–226.

Phillips, P. C. B. and J. Yu (2011). Dating the timeline of financial bubbles during the subprime crisis. *Quantitative Economics 2*(3), 455–491. http://dx.doi.org/10.3982/QE82.

Poledna, S., S. Thurner, J. D. Farmer, and J. Geanakoplos (2014). Leverage-induced systemic risk under Basle II and other credit risk policies. *Journal of Banking & Finance 42*, 199 – 212. https://doi.org/10.1016/j.jbankfin.2014.01.038.

Polkovnichenko, V. and F. Zhao (2013). Probability weighting functions implied in options prices. *Journal of Financial Economics 107*(3), 580 – 609.

Prelec, D. (1998). The probability weighting function. *Econometrica 60*, 497–528.

Quax, R., D. Kandhai, and P. M. Sloot (2013, May). Information dissipation as an early-warning signal for the Lehman Brothers collapse in financial time series. *Scientific Reports 3*. Article no. 1898.

Quiggin, J. (1982). A theory of anticipated utility. *Journal of Economic Behaviour and Organization 3*(4), 323–343.

Quiggin, J. (1993). *Generalized Expected Utility Theory: The Rank Dependent Model*. Boston, MA: Kluwer Academic Press.

Rebaza, J. (2012). *A First Course In Applied Mathematics*. Hobokken, NJ: John Wiley & Sons, Inc.

Resulaj, A., R. Kiani, D. M. Wolpert, and M. N. Shadlen (2009). Changes of mind in decision-making. *Nature 461*(7261), 263–266.

Savadori, L. and L. Mittone (2015). Temporal distance reduces the attractiveness of p-bets compared to \$-bets. *Journal of Economic Psychology 46*(0), 26 – 38.

Schularick, M. and A. M. Taylor (2012, Apr). Credit Booms Gone Bust: Monetary Policy, Leverage Cycles, and Financial Crises, 1870-2008. *American Economic Review 102*(2), 1029–61. http://doi.org/10.1257/aer.102.2.1029.

Serfling, R. J. (1980). *Approximation Theorems of Mathematical Statistics*. New York, NY: John Wiley & Sons.

Shefrin, H. (2016). *The Global Financial Crisis and Its Aftermath: Hidden Factors in the Meltdown*, Chapter 5. Assessing the Contribution of Hyman Minsky's Perspective to Our Understanding of Economic Instability. Oxford, UK: Oxford University Press.

Shefrin, H. and M. Statman (1993). Behavioral aspects of the design and marketing of financial products. *Financial Management 22*(2), 123–134. http://doi.org/10.2307/3665864.

Shintani, M. and O. Linton (2004). Nonparametric neural network estimation of Lyapunov exponents and a direct test for chaos. *Journal of Econometrics 120*(1), 1 – 33.

Shive, S. A. and M. M. Forster (2017). The Revolving Door for Financial Regulators. *Review of Finance 21*(4), 1445–1484. http://dx.doi.org/10.1093/rof/rfw035.

Shorack, G. R. and J. A. Wellner (1986). *Empirical Processes with Applications to Statistics*. New York: John Wiley & Sons, Inc.

Smith, V. L., G. L. Suchanek, and A. W. Williams (1988, Sep). Bubbles, Crashes, and Endogeneous Expectations in Experimental Spot Asset Markets. *Econometrica 56*(5), 1119–1151.

Snowberg, E. and J. Wolfers (2010). Explaining the Favorite–Long Shot Bias: Is It Risk-Love or Misperceptions? *Journal of Political Economy 118*(4), 723–746. https://doi.org/10.1086/655844.

Stiglitz, J. E. and S. J. Grossman (1976). Information and competitive price systems. *American Economic Review 66*(2), 246–253.

Thurner, S., J. D. Farmer, and J. Geanakoplos (2012). Leverage causes fat tails and clustered volatility. *Quantitative Finance 12*(5), 695–707.

Tversky, A. and D. Kahneman (1992). Advances in Prospect Theory: Cumulative Representation of Uncertainty. *Journal of Risk and Uncertainty 5*, 297–323. https://doi.org/10.1007/BF00122574.

Tversky, A. and P. Wakker (1995, Nov.). Risk Attitudes and Decision Weights. *Econometrica 63*(6), 1255–1280.

Wakker, P. A. (2010). *Prospect Theory for Risk and Ambiguity*. New York, NY: Cambridge University Press.

Wang, Y., M. Ding, J. J. Pan, and S. Malone (2017, Oct). Credit Transition Model 2017 Update: Methodology and Performance Reniew. *Moody's Analytics*, 1–31. Available at https://www.moodys.com/sites/products/ProductAttachments/DRD/CTM_Methodology.pdf.

Whang, Y. and O. Linton (1999). The asymptotic distribution of nonparametric estimates of the Lyapunov exponent for stochastic time series. *Journal of Econometrics 91*(1), 1 – 42. http://dx.doi.org/10.1016/S0304-4076(98)00047-5.

White, H. A. (2001). *Asymptotic Theory for Econometricans* (2nd ed.). San Diego, CA: Academic Press, Inc.

Wiggins, S. (2003). *Introduction to Applied Nonlinear Dynamical Systems and Chaos* (2nd ed.), Volume 2 of *Texts in Applied Mathematics*. New York, NY: Springer.

Wigniolle, B. (2014, Apr). Optimism, pessimism and financial bubbles. *Journal of Economic Dynamics and Control 41*, 188–208. https://doi.org/10.1016/j.jedc.2014.01.022.

Yaari, M. (1987, Jan.). The duality theory of choice under risk. *Econometrica 55*(1), 95–115.

Yamazaki, A. (2020). Probability weighting and default risk: A possible explanation for distressed stock puzzles. *Quantitative Finance 20*(5), 745–767. https://doi.org/10.1080/14697688.2019.1698057.

Zhang, R., T. J. Brennan, and A. W. Lo (2014). The origin of risk aversion. *Proceedings of the National Academy of Sciences 111*(50), 17777–17782.

Zhou, W.-X. and D. Sornette (2006). Is there a real-estate bubble in the US? *Physica A: Statistical Mechanics and its Applications 361*(1), 297–308.